

SPIRALLING DYNAMICS NEAR HETEROCLINIC NETWORKS

ALEXANDRE A. P. RODRIGUES AND ISABEL S. LABOURIAU

ABSTRACT. There are few explicit examples in the literature of vector fields exhibiting complex dynamics that may be proved analytically. We construct explicitly a two parameter family of vector fields on the three-dimensional sphere \mathbf{S}^3 , whose flow has a spiralling attractor containing the following: two hyperbolic equilibria, heteroclinic trajectories connecting them transversely and a non-trivial hyperbolic, invariant and transitive set. The spiralling set unfolds a heteroclinic network between two symmetric saddle-foci and contains a sequence of topological horseshoes semiconjugate to full shifts over an alphabet with more and more symbols, coexisting with Newhouse phenomenon. The vector field is the restriction to \mathbf{S}^3 of a polynomial vector field in \mathbf{R}^4 . In this article, we also identify global bifurcations that induce chaotic dynamics of different types.

Keywords:

Heteroclinic network, Spiralling set, Polynomial vector field, Quasistochastic attractor

AMS Subject Classifications:

Primary: 34C28; Secondary: 34C37, 37C29, 37D05, 37G35, 37G40

Address of Alexandre A. P. Rodrigues and Isabel S. Labouriau:
Centro de Matemática da Universidade do Porto
and Faculdade de Ciências, Universidade do Porto
Rua do Campo Alegre, 687, 4169-007 Porto, Portugal
Phone (+351) 220 402 211 and (+351) 220 402 248 Fax (+351) 220 402 209

Date: October 9, 2018.

CMUP is supported by the European Regional Development Fund through the programme COMPETE and by the Portuguese Government through the Fundação para a Ciência e a Tecnologia (FCT) under the project PEst-C/MAT/UI0144/2011. A.A.P. Rodrigues was supported by the grants SFRH/BD/28936/2006 and SFRH/BPD/84709/2012 of FCT.

1. INTRODUCTION

Any C^1 vector field defined on a compact three-dimensional manifold may be approximated by a system of differential equations whose flow exhibits one of the following phenomena: uniform hyperbolicity, a heteroclinic cycle associated to, at least, one equilibrium and/or a homoclinic tangency of the invariant manifolds of the periodic solutions — see Arroyo *et al* [10]. However, there are no examples of vector fields exhibiting all three features simultaneously.

In this article, we construct an explicit example of a C^∞ vector field on the three-dimensional sphere \mathbf{S}^3 that is approximated by differential equations exhibiting all the three behaviours. Nearby differential equations may also display heteroclinic tangencies of invariant manifolds of two equilibria. We describe and characterise some properties of the flow of these differential equations, whose complex geometry arises from spiralling behaviour induced by the presence of saddle-foci. The complex nature of the geometry can be described analytically since our example is close to a highly symmetric vector field that, by construction, exhibits special features. We start with a brief discussion of the literature on examples of this kind.

1.1. Lorenz-like attractors. Few explicit examples of vector fields are known, whose flow contains non-hyperbolic invariant sets that are transitive and for which transitivity is robust to small C^1 perturbations. The most famous example is the expanding *butterfly* proposed by E. Lorenz in 1963 [32] that arises in a flow having an equilibrium at the origin, where the linearisation has eigenvalues $\lambda_u, \lambda_s^1, \lambda_s^2 \in \mathbf{R} \setminus \{0\}$ satisfying:

$$(1.1) \quad \lambda_s^2 < \lambda_s^1 < 0 < \lambda_u \quad \text{and} \quad \lambda_u + \lambda_s^1 > 0.$$

In a three-dimensional manifold, an equilibrium whose linearisation has real eigenvalues satisfying condition (1.1) is what we call an *equilibrium of Lorenz-type*.

In order to understand the Lorenz differential equations and the phenomenon of robust co-existence in the same transitive set of an equilibrium and regular trajectories accumulating on it, geometric models have been constructed independently by Afraimovich *et al* [1] and Guckenheimer and Williams [25]. The construction of these models have been based on properties suggested by numerics.

Morales *et al* [38] unified the theory of uniformly hyperbolic dynamics and Lorenz-like flows stressing that the relevant notion for the general theory of robustly transitive sets is the *dominated splitting*. More precisely, they have proved that if Λ is a robustly transitive attractor containing at least one equilibrium of Lorenz-type, then Λ must be partially hyperbolic with volume expanding directions, up to reversion of time.

In order to make the discussion more rigorous, recall that a compact flow-invariant set Λ is *partially hyperbolic* if, up to time reversal, there is an invariant splitting $T\Lambda = E^s \oplus E^{cu}$ for which there are $K, \lambda \in \mathbf{R}^+$ such that for $\forall t > 0, \forall x \in \Lambda$:

- $\|\partial_x \phi(t, x)|_{E_x^s}\| \leq K e^{-\lambda t}$;
- $\|\partial_x \phi(t, x)|_{E_x^s}\| \cdot \|\partial_x \phi(t, x)|_{E_{\phi(t, x)}^{cu}}\| \leq K e^{-\lambda t}$,

where $\phi(t, p)$ is the unique solution $x(t)$ of the initial value problem $\dot{x} = f(x)$, $x(0) = p$, and $f : \mathbf{R}^4 \rightarrow \mathbf{R}^4$ is a smooth vector field. The direction E^{cu} of Λ is *volume expanding* if

$$\forall t > 0, \quad \forall x \in \Lambda, \quad \det|\partial_x \phi(t, x)|_{E_x^{cu}}| \geq K e^{\lambda t}.$$

The Lorenz model satisfies these conditions. A good explanation about this subject may be found in Araújo and Pacífico [7, Chapter 3], where it is shown that in a three-dimensional manifold the only equilibria that exist near a robustly transitive set must be of Lorenz-type *ie* where condition (1.1) holds — see also Bautista [12].

1.2. Contracting Lorenz Models. In 1981, Arneodo, Couillet and Tresser [8] started the study of *contracting Lorenz models*, whose flows contain attractors that persist only in a measure theoretical sense. The authors considered a variation of the classical Lorenz model with respect to the eigenvalues at the origin, in which the condition (1.1) is replaced by:

$$(1.2) \quad \lambda_s^2 < \lambda_s^1 < 0 < \lambda_u \quad \text{and} \quad \lambda_u + \lambda_s^1 < 0.$$

In 1993, Rovella [45] proved that there exists a *contracting Lorenz model* $\dot{x} = f(x)$, $x \in \mathbf{R}^3$ with an attractor Λ containing an equilibrium so that the following hold: there exists a local basin of attraction \mathcal{B} of Λ , a neighbourhood U of f (in the C^3 -topology) and an open and dense subset $U_0 \subset U$ so that for $\dot{x} = g(x)$ ($g \in U_0$), the maximal invariant set in \mathcal{B} consists of the equilibria, one or two periodic trajectories, a hyperbolic suspended horseshoe and heteroclinic connections. Moreover, Rovella [45] proved that in generic two parameter families $\dot{x} = f(x, \mu)$, with $f(\star, \bar{0}) \equiv f$, there is a set of positive measure containing $\mu = (0, 0)$ for which an attractor in \mathcal{B} containing the equilibrium exists.

The construction of the Rovella attractor [45] is similar to the geometric Lorenz model. Some authors constructed contracting Lorenz-like examples through bifurcations from heteroclinic cycles and networks: for instance, Afraimovich *et al* [2] describe a codimension 1 bifurcation leading from Morse-Smale flows to Lorenz-like attractors; Morales [37] constructed a singular attractor from a hyperbolic flow, through a saddle-node bifurcation. All of these are similar to the expanding Lorenz attractor, for which condition (1.1) hold, as opposed to the contracting case.

1.3. Spiralling attractors. Another type of persistent attractor with a much more complex geometry occurs near homoclinic and heteroclinic cycles associated to either a saddle-focus or a non-trivial periodic solution. This complexity is the reason why the study of this subject was left almost untouched for 20 years from L. P. Shilnikov [47, 48] to P. Holmes [27]. Due to the existence of complex eigenvalues of the linearisations at the equilibria, the spiral structure of the non-wandering set predicted by Arneodo, Couillet and Tresser [9] has been observed in some simulations in the context of the modified Chua's circuit — these attractors are what Aziz-Alaoui [11] call *spiralling attractors*.

Spiralling attractors are expected for perturbations of homo and heteroclinic cycles involving saddle-foci under a dissipative condition. In Kokubu and Roussarie [33], the classic Lorenz model is considered as a particular case of a model whose flow contains a heteroclinic cycle. In this article, the authors carefully choose a perturbation of the classic Lorenz model and have found other types of chaotic dynamics such as Hénon-like chaotic attractors and Lorenz attractors with hooks. There is some evidence that in this case spiral attractors exist and that they might be persistent in the sense of measure [8, 9]. A sequence of topological horseshoes semiconjugate to full shifts on an alphabet with more and more symbols might occur near this kind of attractors.

Nowadays, particular attention is being given to the study of the dynamics near heteroclinic networks with complex behaviour and multispiral attractors. Spiralling dynamics near a large heteroclinic network of rotating nodes has been studied by Aguiar *et al* [4, 5], motivated by a conjecture of Field [18]. A symmetry reduction argument yields a quotient network with two saddle-foci of different Morse indices reminiscent of those studied by Bykov [15, 16]. In [5], the existence of suspended horseshoes with the shape of the network has also been proved.

In a similar context and under the assumption that near the saddle-foci solutions wind in the same direction around the one-dimensional heteroclinic connection, Labouriau and Rodrigues [30] proved the emergence of an intricate behaviour arising in a specific type of symmetry-breaking; no explicit examples have been given. This creates an interest in the construction of explicit vector fields whose flows have a specific type of invariant set and for which it is possible to give an analytical proof of the properties that guarantee the existence of complex behaviour.

In this article, we describe an explicit example of a polynomial vector field on the three-dimensional sphere \mathbf{S}^3 whose flow has a heteroclinic network with two saddle-foci, and a spiralling structure containing a hyperbolic non-trivial transitive set enclosing periodic solutions with different stability indices — this is what Gonchenko *et al* [22] call a quasistochastic attractor. We show that the spiralling set is not robustly transitive, but it presents some similarities to Rovella’s example [45], in the sense that it might be measure-theoretically persistent.

1.4. Heteroclinic terminology. Throughout this paper, by *heteroclinic cycle* we mean a set of finitely many disjoint hyperbolic equilibria p_j (also called *nodes*), $j \in \{1, \dots, k\}$ and trajectories ξ_j , $j \in \{1, \dots, m\}$ such that:

$$\lim_{t \rightarrow +\infty} \xi_j(t) = p_{j+1} = \lim_{t \rightarrow -\infty} \xi_{j+1}(t),$$

called *heteroclinic trajectories*, with the understanding that $\xi_{m+1} = \xi_1$ and $p_{k+1} = p_1$. We also allow connected n -dimensional manifolds of solutions biasymptotic to the nodes p_i and p_j , in negative and positive time, respectively. In both cases we denote the connection by $[p_i \rightarrow p_j]$. Throughout this article, the nodes are hyperbolic; the dimension of the local unstable manifold of an equilibrium p will be called *the Morse index* of p .

A *heteroclinic network* is a connected set that is the union of heteroclinic cycles, where in particular, for any pair of saddles in the network, there is a sequence of heteroclinic connections that links them. Heteroclinic cycles arise robustly in differential equations that are equivariant under the action of a group of symmetries as a connected component of the group orbit of a heteroclinic cycle. We refer the reader to Golubitsky and Stewart [21] for more information about heteroclinic cycles and symmetry in differential equations.

A *Bykov cycle* is a heteroclinic cycle with two saddle-foci of different Morse indices, in which the one-dimensional invariant manifolds coincide and the two-dimensional invariant manifolds have an isolated transverse intersection.

2. THE VECTOR FIELD AND A FRAMEWORK OF THE ARTICLE

2.1. Motivation. It is difficult to find explicit examples for which one can prove that Bykov cycles are present, although these cycles are unavoidable features in one-parameter families of vector fields in three dimensions. Working with vector fields with symmetry simplifies this task in several ways. The most obvious one is that symmetries imply the existence of flow-invariant submanifolds, on which it is easier to find the fragile connection of one-dimensional manifolds. In a two-dimensional flow-invariant set, this may appear as a saddle-to-sink connection, that persists under perturbations that preserve the symmetry. Examples with simple polynomial forms of low degree are natural in symmetric contexts. A simple polynomial form makes computations easier and allows us to prove the transverse intersection of two-dimensional invariant manifolds.

Vector fields that are close to more symmetric ones are easier to analyse, as is done in [4, 5, 30]. In order to illustrate the symmetry breaking reported in [30], we start by defining an organizing center with spherical symmetry whose flow contains an attracting network lying on the unit sphere $\mathbf{S}^3 \subset \mathbf{R}^4$. By gradually breaking the symmetry in a two-parameter family, we obtain a wide range of dynamical phenomena going from sinks to a spiralling structure of suspended horseshoes and cascades of saddle-node bifurcations near a Shilnikov cycle. The construction is amenable to the analytic proof of the features that guarantee the existence of complex behaviour. More precisely, the symmetry-breaking terms have been chosen in such a way that:

- the unit sphere \mathbf{S}^3 remains flow-invariant and globally attracting;
- the cycles persist (although they change their nature);
- the symmetries are broken gradually and independently;

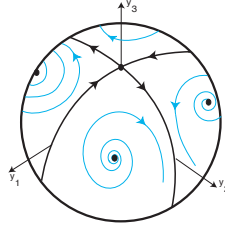


FIGURE 1. Dynamics of the intermediate three-dimensional step in the construction of the organising centre $\mathbf{X}_0(X) = \mathbf{X}(X, 0, 0)$.

- it is possible to show analytically that the two-dimensional invariant manifolds of the nodes meet transversely .

We are interested in dynamics on a compact manifold, in order to have control of the long-time existence and behaviour of solutions.

2.2. The vector field. Our object of study is the two parameter family of vector fields $\mathbf{X}(X, \lambda_1, \lambda_2)$ on the unit sphere $\mathbf{S}^3 \subset \mathbf{R}^4$, defined for $X = (x_1, x_2, x_3, x_4) \in \mathbf{S}^3$ by the differential equation in \mathbf{R}^4 :

$$(2.3) \quad \begin{cases} \dot{x}_1 = x_1(1 - r^2) - x_2 - \alpha_1 x_1 x_4 + \alpha_2 x_1 x_4^2 + \lambda_2 x_3^2 x_4 \\ \dot{x}_2 = x_2(1 - r^2) + x_1 - \alpha_1 x_2 x_4 + \alpha_2 x_2 x_4^2 \\ \dot{x}_3 = x_3(1 - r^2) + \alpha_1 x_3 x_4 + \alpha_2 x_3 x_4^2 + \lambda_1 x_1 x_2 x_4 - \lambda_2 x_1 x_3 x_4 \\ \dot{x}_4 = x_4(1 - r^2) - \alpha_1(x_3^2 - x_1^2 - x_2^2) - \alpha_2 x_4(x_1^2 + x_2^2 + x_3^2) - \lambda_1 x_1 x_2 x_3 \end{cases}$$

where $r^2 = x_1^2 + x_2^2 + x_3^2 + x_4^2$ and $\alpha_2 < 0 < \alpha_1$ with $\alpha_1 + \alpha_2 > 0$.

There are two equilibria given by:

$$\mathbf{v} = (0, 0, 0, +1) \quad \text{and} \quad \mathbf{w} = (0, 0, 0, -1)$$

and the linearisation of $\mathbf{X}(X, \lambda_1, \lambda_2)$ at $(0, 0, 0, \varepsilon)$ with $\varepsilon = \pm 1$ has eigenvalues

$$\alpha_2 - \varepsilon \alpha_1 \pm i \quad \text{and} \quad \alpha_2 + \varepsilon \alpha_1.$$

Then, under the conditions above, \mathbf{v} and \mathbf{w} are hyperbolic saddle-foci, \mathbf{v} has one-dimensional unstable manifold and two-dimensional stable manifold; \mathbf{w} has one-dimensional stable manifold and two-dimensional unstable manifold. The only other equilibrium of (2.3) is the origin.

Equation (2.3) was obtained using a general construction described in Aguiar *et al* [4], that we proceed to summarise in the particular case used here. Start with the differential equation $\dot{Y} = (1 - |Y|^2)Y$ for $Y = (y_1, y_2, y_3) \in \mathbf{R}^3$, for which the unit sphere \mathbf{S}^2 is globally attracting and all its points are equilibria. Then consider a finite subgroup $G \subset \mathbf{O}(3)$ containing

$$d(y_1, y_2, y_3) = (y_1, -y_2, y_3) \quad \text{and} \quad \kappa(y_1, y_2, y_3) = (-y_1, y_2, y_3).$$

The second step is to add two G -symmetric perturbing terms, $\alpha_1 A(Y)$ and $\alpha_2 B(Y)$, to the differential equation. The two terms are chosen to be tangent to \mathbf{S}^2 , so this sphere is still flow-invariant. From the symmetry, it follows that the two planes $\{d(Y) = Y\}$ and $\{\kappa(Y) = Y\}$ are also flow-invariant and the dynamics is that of Figure 1.

Now, add the equation $\dot{\theta} = 1$ and interpret (θ, y_1) as polar coordinates in \mathbf{R}^2 . In the new variables $(x_1, x_2, x_3, x_4) = (y_1 \cos \theta, y_1 \sin \theta, y_2, y_3)$ this is equation (2.3) for $\lambda_1 = \lambda_2 = 0$, so, by construction, the unit sphere \mathbf{S}^3 is invariant under the flow of (2.3) for $\lambda_1 = \lambda_2 = 0$ and every trajectory with nonzero initial condition is asymptotic to it in forward time. Hence, (2.3) defines a family of vector fields $\mathbf{X}(X, 0, 0)$ on \mathbf{S}^3 . The invariant circle $\{d(Y) = Y\}$ gives rise to an invariant two-sphere and $\{\kappa(Y) = Y\}$ gives rise to an invariant circle.

Other properties of (2.3) with $\lambda_1 = \lambda_2 = 0$ that follow by construction, are given Aguiar *et al* [4, Theorem 10], we describe them briefly.

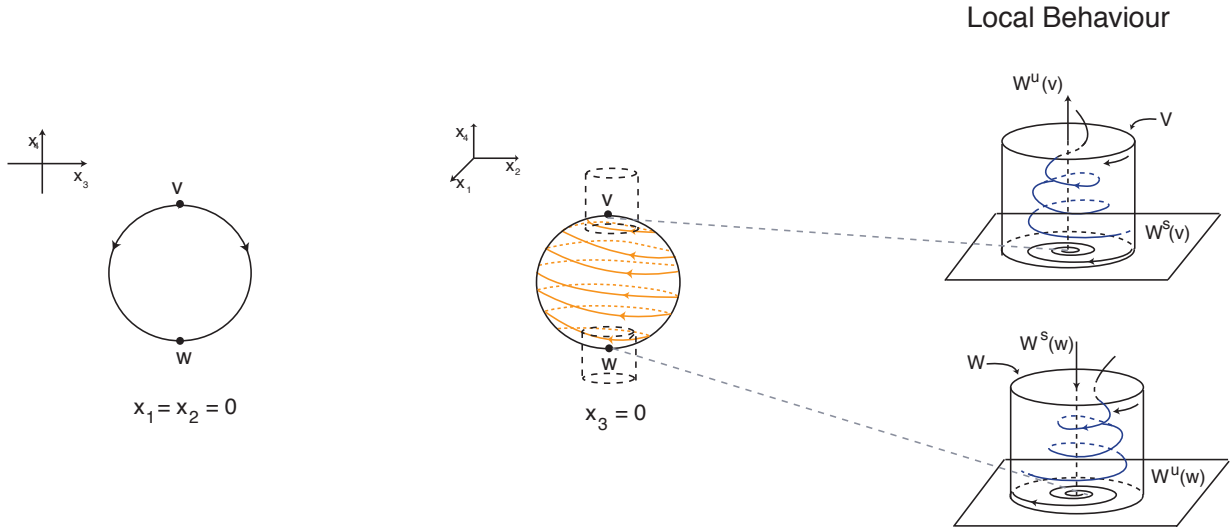


FIGURE 2. Dynamics of the organising centre $\mathbf{X}_0(X) = \mathbf{X}(X, 0, 0)$. Left: The one-dimensional heteroclinic connection from \mathbf{v} to \mathbf{w} on the invariant circle $Fix(\mathbf{SO}(2)) \cap \mathbf{S}^3$. Centre: The two-dimensional heteroclinic connection from \mathbf{w} to \mathbf{v} on the invariant two-sphere $Fix(\mathbf{Z}_2(\gamma_2)) \cap \mathbf{S}^3$. Right: Open neighbourhoods of \mathbf{v} and \mathbf{w} , inside which the direction of solutions turning around the connection $[\mathbf{v} \rightarrow \mathbf{w}]$ is the same.

The group of symmetries of $\mathbf{X}_0(X) = \mathbf{X}(X, 0, 0)$ is isomorphic to $\mathbf{SO}(2) \oplus \mathbf{Z}_2(\gamma_2)$ where $\psi_\theta \in \mathbf{SO}(2)$ acts as:

$$\psi_\theta(x_1, x_2, x_3, x_4) = (x_1 \cos \theta - x_2 \sin \theta, x_1 \sin \theta + x_2 \cos \theta, x_3, x_4)$$

and $\gamma_2 \in \mathbf{Z}_2(\gamma_2)$ acts as:

$$\gamma_2(x_1, x_2, x_3, x_4) = (x_1, x_2, -x_3, x_4).$$

This comes from the symmetry group G , plus the rotation into \mathbf{R}^4 .

The one-dimensional invariant manifolds of \mathbf{v} and \mathbf{w} lie inside the invariant circle $Fix(\mathbf{SO}(2)) \cap \mathbf{S}^3$ and the two-dimensional invariant manifolds lie in the invariant two-sphere $Fix(\mathbf{Z}_2(\gamma_2)) \cap \mathbf{S}^3$. Thus, symmetry forces the invariant manifolds of \mathbf{v} and \mathbf{w} to be in a very special position: they coincide, see Figure 2. The two saddle-foci, together with their invariant manifolds form a heteroclinic network Σ^0 that is asymptotically stable by the criteria of Krupa and Melbourne [34, 35]. Indeed since $\alpha_2 < 0 < \alpha_1$, it follows that:

$$\rho = \frac{C_{\mathbf{v}} C_{\mathbf{w}}}{E_{\mathbf{v}} E_{\mathbf{w}}} = \left(\frac{\alpha_2 - \alpha_1}{\alpha_2 + \alpha_1} \right)^2 > 1,$$

where E_p and C_p denote the real parts of the expanding and contracting eigenvalues of DX_0 at p , where $p \in \{\mathbf{v}, \mathbf{w}\}$.

The network Σ^0 can be decomposed into two cycles. Due to the symmetry and to the asymptotic stability, trajectories whose initial condition starts outside the invariant fixed point subspaces will approach in positive time one of the cycles. The fixed point hyperplanes prevent random visits to the two cycles; a trajectory that approaches one of the cycles in Σ^0 is shown in Figure 3. The time series of the figure shows the increasing intervals of time spent near the equilibria. The sejour time in any neighbourhood of one of saddle-foci increases geometrically with ratio ρ .

2.3. Symmetry breaking along the article. The symmetries of the organising centre are broken when either λ_1 or λ_2 is not zero. This was done by adding two terms $\lambda_1 F_1(X)$ and $\lambda_2 F_2(X)$ that break the $\mathbf{SO}(2) \oplus \mathbf{Z}_2(\gamma_2)$ symmetry in different ways — see Appendix B. Both

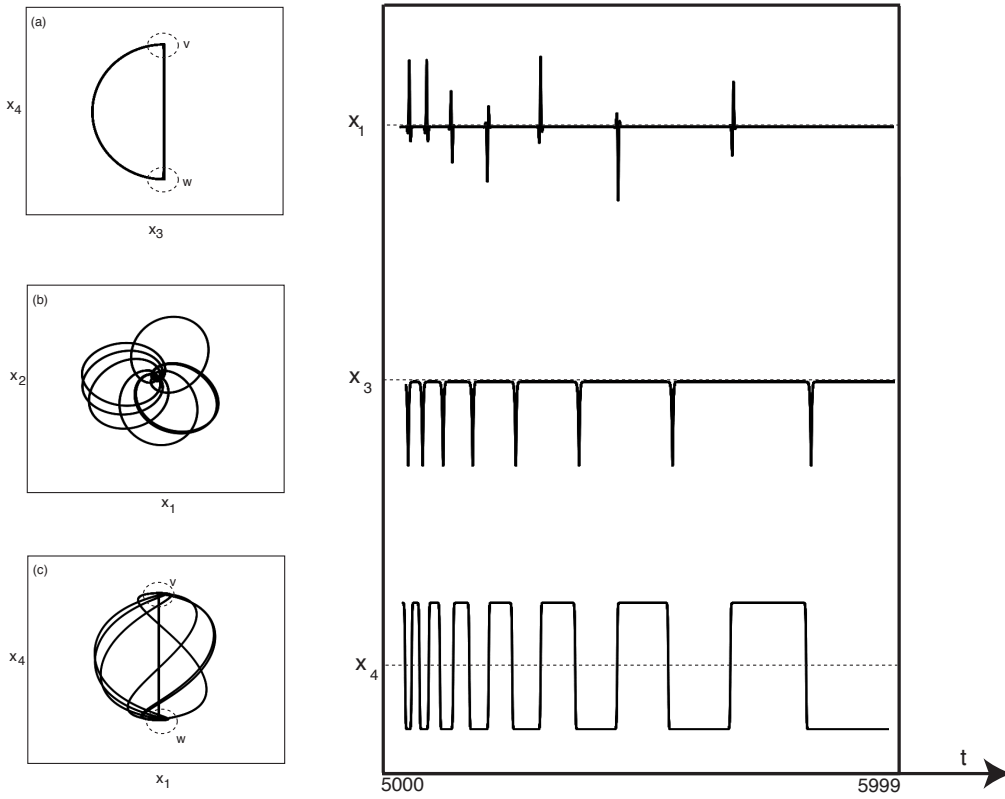


FIGURE 3. Left: Projection in the (x_3, x_4) , (x_1, x_2) and (x_1, x_4) -planes of the trajectory with initial condition $(-0.5000, -0.1390, -0.8807, 0.3013)$ for the flow corresponding to $\mathbf{X}_0(X) = \mathbf{X}(X, 0, 0)$, with $\alpha_1 = 1$, $\alpha_2 = -0.1$. Right: Corresponding time series. The simulations omit the initial transient (the independent variable t varies between 5000 and 5999).

F_1 and F_2 are chosen to be tangent to \mathbf{S}^3 , therefore $\mathbf{X}(X, \lambda_1, \lambda_2)$ is still a well defined vector field on \mathbf{S}^3 .

In Section 3, after some additional results on $\mathbf{X}_0(X)$, we discuss briefly the dynamics of $\mathbf{X}(X, 0, \lambda_2)$, with $\lambda_2 \neq 0$, when the rotational symmetry $\mathbf{SO}(2)$ is broken, destroying the network Σ^0 . Then we exploit the more dynamically interesting situation that arises for $\lambda_1 \neq 0$ and $\lambda_2 = 0$. In this case the reflection symmetry \mathbf{Z}_2 is broken, as well as part of the $\mathbf{SO}(2)$ -symmetry. The two-dimensional connection breaks into a pair of one-dimensional ones, but due to the remaining symmetry, the one-dimensional connections from \mathbf{v} to \mathbf{w} are preserved. This gives rise to two Bykov cycles. Analytical proof of transverse intersection of two invariant manifolds is usually difficult to obtain but this can be achieved in our example, and is done in Appendix A. Similar heteroclinic bifurcations have been studied in the context of a model of the long Josephson junction [13].

When both λ_1 and λ_2 are non zero, all the symmetry is broken, hence the one-dimensional connection from \mathbf{v} to \mathbf{w} disappears. Although the attracting heteroclinic cycles disappears, some nearby attracting structures remain, this is discussed in Section 4. Our results and conjectures are illustrated by numerical simulations, which have been obtained using *Matlab* and the dynamical systems package *Dstool*.

3. PARTIAL SYMMETRY BREAKING

The existence of the attracting heteroclinic network Σ^0 for \mathbf{X}_0 requires two separate symmetries to allow structurally stable connections within the two invariant fixed point subspaces. Throughout this paper, we control the degree to which the two symmetries are broken by two parameters, λ_1 and λ_2 : λ_1 controls the magnitude of the $\mathbf{SO}(2) \times \mathbf{Z}_2(\gamma_2)$ -symmetry-breaking term and λ_2 controls the breaking of the pure reflectional symmetry $\mathbf{Z}_2(\gamma_1)$ where $\gamma_1 = \Psi_\pi \in \mathbf{SO}(2)$, $\gamma_1(x_1, x_2, x_3, x_4) = (-x_1, -x_2, x_3, x_4)$. The parameters λ_1 and λ_2 play exactly the same role as in [30].

Before discussing the effects of breaking the symmetry in (2.3) when either λ_1 or λ_2 is non zero, we need some additional information on the fully symmetric case.

3.1. The organising centre. For \mathbf{X}_0 , there are two possibilities for the geometry of the flow around each saddle-focus of the network Σ^0 , depending on the direction solutions turn around $[\mathbf{v} \rightarrow \mathbf{w}]$, as discussed in Labouriau and Rodrigues [30]. The next proposition shows that each solution when close to \mathbf{v} turns in the same direction as when close to \mathbf{w} .

Proposition 1. *In \mathbf{S}^3 , there are open neighbourhoods V and W of \mathbf{v} and \mathbf{w} , respectively, such that, for any trajectory of \mathbf{X}_0 going from V to W , the direction of its turning around the connection $[\mathbf{v} \rightarrow \mathbf{w}]$ is the same in V and in W .*

Proof. The explicit expression of \mathbf{X}_0 in spherical coordinates is the special case $\lambda_1 = 0$ of equation (A.8) in Appendix A. The equation for the angular coordinate φ in the plane $(x_1, x_2, 0, 0)$ is $\dot{\varphi} = 1$. Since this plane is perpendicular to $Fix(\mathbf{SO}(2)(\gamma_1))$, where the connection $[\mathbf{v} \rightarrow \mathbf{w}]$ lies, trajectories must turn around the connection in the same direction. \square

The property in Proposition 1 is persistent under *isotopies*: if it holds for the organising centre $\lambda_1 = \lambda_2 = 0$, then it is still valid in smooth one-parameter families containing it, as long as there is still a connection. In particular, Property (P8) of [30] is verified and thus their results may be applied to the present work.

3.2. Breaking the two-dimensional heteroclinic connection. For $\lambda_1 \neq 0$, the vector field $\mathbf{X}_1(X) = \mathbf{X}(X, \lambda_1, 0)$ is no longer $\mathbf{SO}(2) \oplus \mathbf{Z}_2(\gamma_2)$ but is still equivariant under the action of $\gamma_1 \in \mathbf{SO}(2)$. This breaks the two-dimensional connection $[\mathbf{w} \rightarrow \mathbf{v}]$ into a transverse intersection of invariant manifolds.

Theorem 2. *The vector field $\mathbf{X}_1(X) = \mathbf{X}(X, \lambda_1, 0)$ on \mathbf{S}^3 has symmetry group $\mathbf{Z}_2(\gamma_1)$ and for small $\lambda_1 \neq 0$ its flow has a heteroclinic network Σ^* involving the two equilibria \mathbf{v} and \mathbf{w} with the following properties:*

- (1) *there are two one-dimensional heteroclinic connections from \mathbf{v} to \mathbf{w} inside $Fix(\mathbf{Z}_2(\gamma_1)) \cap \mathbf{S}^3$;*
- (2) *there are no homoclinic connections to the equilibria;*
- (3) *the two-dimensional invariant manifolds of \mathbf{v} and \mathbf{w} intersect transversely along one-dimensional connections from \mathbf{w} to \mathbf{v} .*

The connections from \mathbf{v} to \mathbf{w} persist under small perturbations that preserve the γ_1 -symmetry.

The new network Σ^* is qualitatively different from Σ^0 . The transversality of the unstable manifold of \mathbf{w} , $W^u(\mathbf{w})$, and the stable manifold of \mathbf{v} , $W^s(\mathbf{v})$, and the persistence of the heteroclinic connections from \mathbf{v} to \mathbf{w} give rise to a *Bykov cycle*. In a non-symmetric context, Bykov cycles arise as bifurcations of codimension 2, the points in parameter space where they appear are called *T-points* in [20] — see Figure 4.

The existence of a Bykov cycle implies the existence of a bigger network: beyond the original transverse connections, there are infinitely many subsidiary heteroclinic connections turning

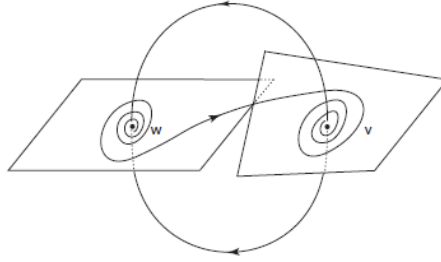


FIGURE 4. Bykov cycle Σ^* : heteroclinic cycle associated to two saddle-foci of different Morse indices, in which the one-dimensional invariant manifolds coincide and the two-dimensional invariant manifolds intersect transversely .

around the original Bykov cycle, that have the same bifurcation structure in their unfolding. Multi-pulses are also expected.

Proof of Theorem 2. Clearly the perturbation term breaks all the symmetries of $\mathbf{X}_1(X)$ except γ_1 . It is also immediate that $\gamma_1(\mathbf{v}) = \mathbf{v}$, $\gamma_1(\mathbf{w}) = \mathbf{w}$. The circle $Fix(\mathbf{Z}_2(\gamma_1)) \cap \mathbf{S}^3$ is still flow-invariant and contains no other equilibria, thus it still consists of the two equilibria \mathbf{v} and \mathbf{w} and the two connections from \mathbf{v} to \mathbf{w} . The plane $Fix(\mathbf{Z}_2(\gamma_1))$ will remain invariant under any perturbation that preserves the symmetry. Since on this plane \mathbf{v} is a saddle and \mathbf{w} is a sink, the connection persists under small perturbations.

Since \mathbf{v} and \mathbf{w} are hyperbolic, $Fix(\mathbf{Z}_2(\gamma_1)) \supset [\mathbf{v} \rightarrow \mathbf{w}]$ and $\dim W^u(\mathbf{v}) = \dim W^s(\mathbf{w}) = 1$, item (2) follows. Breaking the $\mathbf{Z}_2(\gamma_2)$ -equivariance is necessary for the existence of transverse intersection of the manifolds $W^u(\mathbf{w})$ and $W^s(\mathbf{v})$. Nevertheless, the manifolds could intersect non transversely . The proof of transversality of the intersection of the two-dimensional manifolds, using the Melnikov method is similar to that given in Aguiar *et al* [4]. For completeness, we give the proof in Appendix A. \square

Hereafter, our main goal is the description of the spiralling set that appears in the flow of \mathbf{X}_1 . First, we establish some results and terminology about the local and global dynamics. We follow closely the general results in [6, 30, 41] this is why proofs are short. More details are given in these references.

3.2.1. Local and global dynamics. By Theorem 2, the unfolding $\mathbf{X}_1 = \mathbf{X}(X, \lambda_1, 0) : \mathbf{S}^3 \rightarrow \mathbf{TS}^3$ of \mathbf{X}_0 is a family of C^1 vector fields such that for $\lambda_1 \neq 0$, the local two-dimensional manifolds $W^u(\mathbf{w})$ and $W^s(\mathbf{v})$ intersect transversely at (at least) two trajectories. In order to describe the dynamics around the Bykov cycles, we introduce local coordinates near the saddle-foci \mathbf{v} and \mathbf{w} and we define some terminology.

Since $C_{\mathbf{v}} \neq E_{\mathbf{v}}$ and $C_{\mathbf{w}} \neq E_{\mathbf{w}}$, then by Samovol [46], the vector field \mathbf{X}_1 is C^1 -conjugate to its linear part around each saddle-focus. Linearisation may fail under resonance conditions that correspond to curves in the (α_1, α_2) -plane. This restriction has zero Lebesgue measure, and thus it does not place serious constraint on our analysis. In cylindrical coordinates (ρ, θ, z) the linearisation at \mathbf{v} takes the form:

$$\dot{\rho} = -C_{\mathbf{v}}\rho \quad \dot{\theta} = 1 \quad \dot{z} = E_{\mathbf{v}}z$$

and around \mathbf{w} it is given by:

$$\dot{\rho} = E_{\mathbf{w}}\rho \quad \dot{\theta} = 1 \quad \dot{z} = -C_{\mathbf{w}}z.$$

After a linear rescaling of the local variables, we consider cylindrical neighbourhoods $V \subset \mathbf{S}^3$ and $W \subset \mathbf{S}^3$ of \mathbf{v} and \mathbf{w} , of radius 1 and height 2, respectively. We suggest that the reader follows this section observing Figure 5.

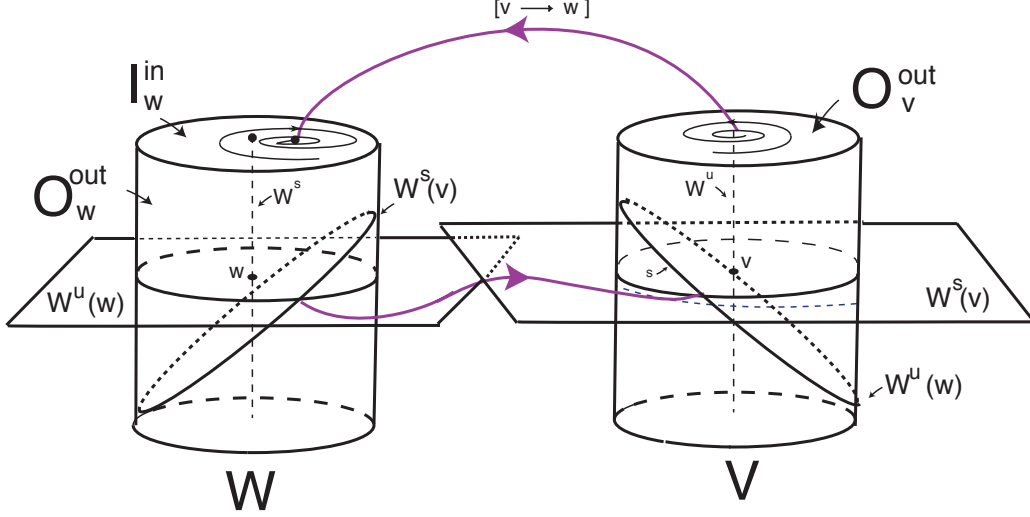


FIGURE 5. Conventions in the cylindrical neighbourhoods of \mathbf{v} and \mathbf{w} . Both $W_{loc}^s(\mathbf{v}) \cap O_{\mathbf{w}}^{out}$ and $W_{loc}^u(\mathbf{w}) \cap O_{\mathbf{v}}^{in}$ are closed curves in the boundaries of the cylinders for small values of $\lambda_1 \neq 0$.

The boundary of each cylinder forms an *isolating block*. It consists of three components: the cylinder wall parametrised by $x \in \mathbf{R} \pmod{2\pi}$ and $|y| \leq 1$ with the usual cover $(x, y) \mapsto (1, x, y) = (\rho, \theta, z)$ and two discs, the top and bottom of the cylinder. Choosing coordinates so that one of the connections $[\mathbf{v} \rightarrow \mathbf{w}]$ joins the tops of the two cylinders, we may from now on restrict our attention to the upper part of the walls $y \geq 0$ and the tops of the cylinders, behaviour at the bottom is obtained by symmetry. We take polar coverings of the top discs $(r, \varphi) \mapsto (r, \varphi, 1) = (\rho, \theta, z)$ with $0 \leq r \leq 1$ with $\varphi \in \mathbf{R} \pmod{2\pi}$ and let:

- $O_{\mathbf{v}}^{out}$ be the top of the cylinder V , where the flow goes out of V ;
- $I_{\mathbf{v}}^{in}$ be the upper part of the wall of the cylinder V , where the flow goes in V ;
- $O_{\mathbf{w}}^{out}$ be the upper part of the wall of the cylinder W , where the flow goes out of W ;
- $I_{\mathbf{w}}^{in}$ be the top of the cylinder W , where the flow goes in W .

The trajectories of all points (x, y) in $I_{\mathbf{v}}^{in} \setminus W^s(\mathbf{v})$, leave V at $O_{\mathbf{v}}^{out}$ at

$$(3.4) \quad \Phi_{\mathbf{v}}(x, y) = \left(y^{\delta_{\mathbf{v}}}, -\frac{\ln y}{E_{\mathbf{v}}} + x \right) = (r, \phi) \quad \text{where} \quad \delta_{\mathbf{v}} = \frac{C_{\mathbf{v}}}{E_{\mathbf{v}}}.$$

Similarly, points (r, ϕ) in $I_{\mathbf{w}}^{in} \setminus W^s(\mathbf{w})$, leave W at $O_{\mathbf{w}}^{out}$ at

$$(3.5) \quad \Phi_{\mathbf{w}}(r, \phi) = \left(-\frac{\ln r}{E_{\mathbf{w}}} + \phi, r^{\delta_{\mathbf{w}}} \right) = (x, y) \quad \text{where} \quad \delta_{\mathbf{w}} = \frac{C_{\mathbf{w}}}{E_{\mathbf{w}}}.$$

The transition between cylinders follows each connection in a flow-box. The flow sends points in $O_{\mathbf{v}}^{out}$ near $W_{loc}^u(\mathbf{v})$ into $I_{\mathbf{w}}^{in}$ along the connection $[\mathbf{v} \rightarrow \mathbf{w}]$ defining a transition map $\Psi_{\mathbf{v} \rightarrow \mathbf{w}} : O_{\mathbf{v}}^{out} \rightarrow I_{\mathbf{w}}^{in}$ that we may assume to be the identity. There is also a well defined transition map $\Psi_{\mathbf{w} \rightarrow \mathbf{v}} : O_{\mathbf{w}}^{out} \rightarrow I_{\mathbf{v}}^{in}$ that can be taken to be a rotation [30]. We choose our coordinates to have the connection $[\mathbf{w} \rightarrow \mathbf{v}]$ meeting $I_{\mathbf{v}}^{in}$ and $O_{\mathbf{w}}^{out}$ at $(x, y) = (0, 0)$.

Let $\eta := \Phi_{\mathbf{w}} \circ \Psi_{\mathbf{v} \rightarrow \mathbf{w}} \circ \Phi_{\mathbf{v}}$ and define the first return map to $I_{\mathbf{v}}^{in}$ as $\Psi := \Psi_{\mathbf{w} \rightarrow \mathbf{v}} \circ \eta$ at all points where it is well defined.

The geometry of the local transition maps is described using the following terminology: a *segment* β on $I_{\mathbf{v}}^{in}$ is a smooth regular parametrised curve $\beta : [0, 1) \rightarrow I_{\mathbf{v}}^{in}$ that meets $W_{loc}^s(\mathbf{v})$ transversely at the point $\beta(1)$ only and such that, writing $\beta(s) = (x(s), y(s))$, both x and y are monotonic functions of s .

A *spiral* on a disc D around a point $p \in D$ is a curve $\alpha : [0, 1) \rightarrow D$ satisfying $\lim_{s \rightarrow 1^-} \alpha(s) = p$ and such that if $\alpha(s) = (r(s), \theta(s))$ is its expressions in polar coordinates around p then the maps r and θ are monotonic, and $\lim_{s \rightarrow 1^-} |\theta(s)| = +\infty$.

Consider a cylinder C parametrised by a covering $(\theta, h) \in \mathbf{R} \times [a, b]$, with $a < b \in \mathbf{R}$ where θ is periodic. A *helix* on the cylinder C *accumulating on the circle* $h = h_0$ is a curve $\alpha : [0, 1) \rightarrow C$ such that its coordinates $(\theta(s), h(s))$ satisfy $\lim_{s \rightarrow 1^-} h(s) = h_0$, $\lim_{s \rightarrow 1^-} |\theta(s)| = +\infty$ and the maps θ and h are monotonic. Using these definitions and the expressions (3.4) and (3.5) for $\Phi_{\mathbf{v}}$ and $\Phi_{\mathbf{w}}$ we get:

Proposition 3 (Aguiar *et al* [6], 2010). *A segment on $I_{\mathbf{v}}^{in}$ is mapped by $\Phi_{\mathbf{v}}$ into a spiral on $O_{\mathbf{w}}^{out}$ around $W_{loc}^u(\mathbf{v}) \cap Out(\mathbf{v})$. This spiral is mapped by $\Psi_{\mathbf{v} \rightarrow \mathbf{w}}$ into another spiral around $W_{loc}^s(\mathbf{w}) \cap I_{\mathbf{v}}^{in}$, which is mapped by $\Phi_{\mathbf{w}}$ into a helix on $O_{\mathbf{w}}^{out}$ accumulating on the circle $O_{\mathbf{w}}^{out} \cap W^u(\mathbf{w})$.*

3.2.2. The spiralling set. The study of “routes to chaos” has been a recurring concern in the research on nonlinear dynamics during the last decades. Several patterns have been described for qualitative changes in features of vector fields that vary under small changes of a one-dimensional parameter. In the present research, when λ_1 moves away from zero, we observe a phenomenon called *instant chaos* in different contexts [17, 24, 29]: an instantaneous jump from a regular flow near Σ^* to chaotic behaviour, with suspended horseshoes and homoclinic classes.

Theorem 4. *For generic $\alpha_1 \neq \alpha_2$ and for any small $\lambda_1 \neq 0$, the vector field $\mathbf{X}_1 = \mathbf{X}(X, \lambda_1, 0)$ is $\mathbf{Z}_2(\gamma_1)$ -equivariant and its flow has a compact spiralling set $\Lambda \subset \mathbf{S}^3$ containing the heteroclinic network Σ^* of Theorem 2, involving the saddle-foci \mathbf{v} and \mathbf{w} with a transverse intersection of the two-dimensional invariant manifolds; and moreover the suspension of a compact set $\mathcal{H} = \bigcup_{i \in \mathbf{Z}} \mathcal{H}_i \subset I_{\mathbf{v}}^{in}$, where $\{\mathcal{H}_i\}_{i \in \mathbf{Z}}$ is an increasing sequence of invariant sets, accumulating on Σ^* . The dynamics of the first return map Ψ to \mathcal{H} is uniformly hyperbolic and topologically conjugate to the suspension of a full shift over an infinite set of symbols.*

Proof. The existence of the network Σ^* follows from Theorem 2. For $\lambda_1 = 0$, the heteroclinic network Σ^0 for \mathbf{X}_0 is asymptotically stable. In particular, there are arbitrarily small compact neighbourhoods of Σ^0 such that the vector field is transverse to their boundaries where it points inwards. Let \mathcal{N} be one of these neighbourhoods. There exists $\lambda_* > 0$ such that for $\lambda_1 < \lambda_*$, the vector field \mathbf{X}_1 is still transverse to the boundary of \mathcal{N} and $\Sigma^* \subset \mathcal{N}$. Thus \mathcal{N} is a compact set that is positively invariant under the flow of \mathbf{X}_1 . Hence \mathcal{N} contains an attractor.

We use the ideas of [5, 6, 41] adapted to our purposes to show the existence of the suspended horseshoe accumulating on the heteroclinic network (see Figure 6). We start by taking cylindrical neighbourhoods V and W of each equilibrium as in 3.2.1.

For small $\varepsilon > 0$ and $\tau \in (0, 1]$, consider the rectangles $R_{\mathbf{v}} \subset I_{\mathbf{v}}^{in}$ and $R_{\mathbf{w}} \subset O_{\mathbf{w}}^{out}$ parametrised by $(x, y) \in [-\varepsilon, \varepsilon] \times [0, \tau]$. Let β be a vertical segment in $R_{\mathbf{v}}$ whose angular component is $x_0 \in (-\varepsilon, \varepsilon)$, lying across the stable manifold of \mathbf{v} . By Proposition 3, its image by $\Phi_{\mathbf{v}}$ accumulates as a spiral on the unstable manifold of \mathbf{v} that is then mapped by $\Psi_{\mathbf{v} \rightarrow \mathbf{w}}$ into another spiral accumulating on the stable manifold of \mathbf{w} — see Figure 6. This spiral of initial conditions on $I_{\mathbf{v}}^{in}$ is mapped, by the local map near \mathbf{w} , into points lying on a helix in $O_{\mathbf{w}}^{out}$ that accumulates on $W_{loc}^u(\mathbf{w}) \cap O_{\mathbf{w}}^{out}$. On the other hand, the curve $W_{loc}^s(\mathbf{v}) \cap O_{\mathbf{w}}^{out}$ is a segment in $O_{\mathbf{w}}^{out}$, hence the helix crosses it transversely infinitely many times. The composition of consecutive local maps and transition functions transforms the original segment β of initial conditions lying across $W^s(\mathbf{v})$ into infinitely many segments in $R_{\mathbf{v}}$ with the same property.

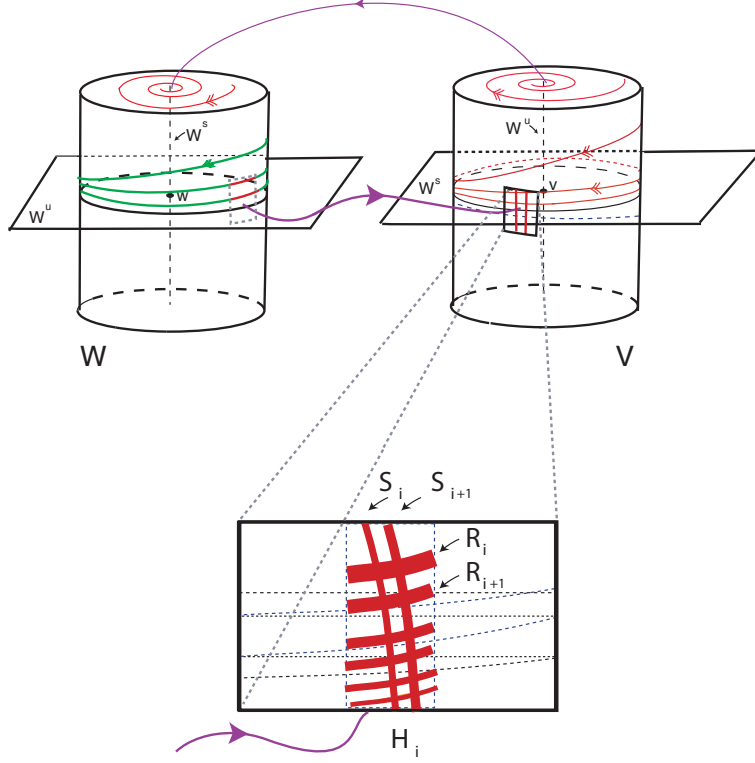


FIGURE 6. Construction of the suspended horseshoe \mathcal{H}_i for \mathbf{X}_1 near the cycle, giving rise to the Cantor set on the wall of the cylinder, generated by an arbitrarily large number of strips.

Proposition 5 of [41] shows that there are $n_0 \in \mathbf{N}$ and a family of intervals $(\mathcal{I}_n)_{n \geq n_0} = ([e^{a_n}, e^{b_n}])_{n \geq n_0}$, where:

$$a_n = K^{-1}(-\varepsilon - 2n\pi + x_0), \quad b_n = K^{-1}(\varepsilon - 2n\pi + x_0) \quad \text{and} \quad K = \frac{C_v + E_w}{E_v E_w} > 0,$$

such that $\beta([e^{a_n}, e^{b_n}]) \subset I_v^{in}$ and $\eta \circ \beta([e^{a_n}, e^{b_n}]) \subset R_w$. Since a_n and b_n depend smoothly on the angular coordinate x_0 of the vertical segment β , then the sequence of horizontal strips:

$$\mathcal{R}_n = [-\varepsilon, \varepsilon] \times \beta([e^{a_n(x_0)}, e^{b_n(x_0)}]) \subset R_v, \quad n \geq n_0 \in \mathbf{N}, \quad x \in [-\varepsilon, \varepsilon]$$

is mapped by η onto R_w . The image under η of the endpoints of the horizontal boundaries of \mathcal{R}_n must join the end points of $\eta([e^{a_n}, e^{b_n}]) \subset R_w$; since the map $\Psi_{w \rightarrow v}$ is assumed to be a rotation, for each $n > n_0$, the horizontal strip \mathcal{R}_n is mapped by Ψ into a vertical strip \mathcal{S}_n across $R_v \subset I_v^{in}$.

Moreover, the set $\bigcap_{k \in \mathbf{Z}} \left(\bigcup_{i=1}^k \Psi^i(\mathcal{R}_i) \right)$ is a Cantor set of initial conditions where the return map to $\bigcup_{i \in \mathbf{N}} \mathcal{R}_i$ is well defined both in forward and in backward time, for arbitrarily large times. The dynamics of Ψ restricted to the above invariant set is semi-conjugate to a full shift over

an infinite alphabet that represents the paths in Σ^* . In [5], it is shown that if Π is a transverse section to the suspended horseshoe \mathcal{H} , the first return map to Π is hyperbolic at all points where it is well defined. \square

Points lying on the invariant manifolds of \mathbf{v} and \mathbf{w} are dense in the suspended horseshoe \mathcal{H} . In particular, the *topological entropy* of the corresponding flow is positive. The set \mathcal{H} might have positive Lebesgue measure like the “fat Bowen horseshoe”. Using the Conley-Moser Conditions, Rodrigues [41] proved that the shift dynamics does not trap most trajectories that remain in a small neighbourhood of Σ^* :

Corollary 5. *Let N^{Σ^*} be a tubular neighbourhood of one of the Bykov cycles Σ^* . Then, in any cross-section $\Pi_q \subset N^{\Sigma^*}$ at a point q in $[\mathbf{w} \rightarrow \mathbf{v}]$, the set of initial conditions in $\Pi_q \cap N^{\Sigma^*}$ that do not leave N^{Σ^*} for all time has zero Lebesgue measure.*

3.2.3. Heteroclinic Switching and Subsidiary Dynamics. One astonishing property is the possibility of shadowing the heteroclinic network Σ^* by the property called *heteroclinic switching*: any infinite sequence of pseudo-orbits defined by admissible heteroclinic connections can be shadowed, as we proceed to define.

For the heteroclinic network Σ^* with node set $\{\mathbf{v}, \mathbf{w}\}$, a *path of order k* on Σ^* is a finite sequence $s^k = (c_j)_{j \in \{1, \dots, k\}}$ of heteroclinic connections $c_j = [A_j \rightarrow B_j]$ in Σ^* such that $A_j, B_j \in \{\mathbf{v}, \mathbf{w}\}$ and $B_j = A_{j+1}$. An infinite path corresponds to an infinite sequence of connections in Σ^* . Let N_{Σ^*} be a neighbourhood of the network Σ^* and let U_A be a neighbourhood of a node A . For each heteroclinic connection in Σ^* , consider a point p_i on it and a small neighbourhood V_i of p_i . We assume that the neighbourhoods of the nodes are pairwise disjoint, as well for those of points in connections.

Given neighbourhoods as before, the trajectory $\phi(t, q)$, follows the finite path $s^k = (c_j)_{j \in \{1, \dots, k\}}$ of order k , if there exist two monotonically increasing sequences of times $(t_i)_{i \in \{1, \dots, k+1\}}$ and $(z_i)_{i \in \{1, \dots, k\}}$ such that for all $i \in \{1, \dots, k\}$, we have $t_i < z_i < t_{i+1}$ and:

- (1) $\phi(t, q) \subset N_{\Sigma^*}$ for all $t \in (t_1, t_{k+1})$;
- (2) $\phi(t_i, q) \in U_{A_i}$ and $\phi(z_i, q) \in V_i$ and
- (3) for all $t \in (z_i, z_{i+1})$, $\phi(t, q)$ does not visit the neighbourhood of any other node except that of A_{i+1} .

There is *finite switching* near Σ^* if for each finite path there is a trajectory that follows it. Analogously, we define *infinite switching* near Σ^* if every forward infinite sequence of connections in the network is shadowed by nearby trajectories.

Infinite switching near Σ^* follows from the proof of Theorem 4 and the results of Aguiar *et al* [6]. The solutions that realise switching lie in a tubular neighbourhood N^{Σ^*} of Σ^* , hence from the results of Rodrigues [41], it follows that:

Corollary 6. *There is a set of initial conditions with positive Lebesgue measure for which there is finite switching near the network Σ^* . There is also infinite switching, realised by a set of initial conditions with zero Lebesgue measure.*

The complex eigenvalues force the spreading of solutions around the unstable manifold of \mathbf{w} , allowing visits to all possible connections starting at \mathbf{w} . The transversality enables the existence of solutions that follow heteroclinic connections on the two different connected components of $S^3 \setminus W_{loc}^s(\mathbf{v})$, the upper and the lower part on the wall of the cylinder — see Figure 6.

From the results of [30], it also follows that near Σ^* the only heteroclinic connections from \mathbf{v} to \mathbf{w} are the original ones and that the finite switching near Σ^* may be realised by an n -pulse heteroclinic connection $[\mathbf{w} \rightarrow \mathbf{v}]$. Moreover, among all the solutions which appear in \mathcal{H} , there are infinitely many knot types, inducing all link types.

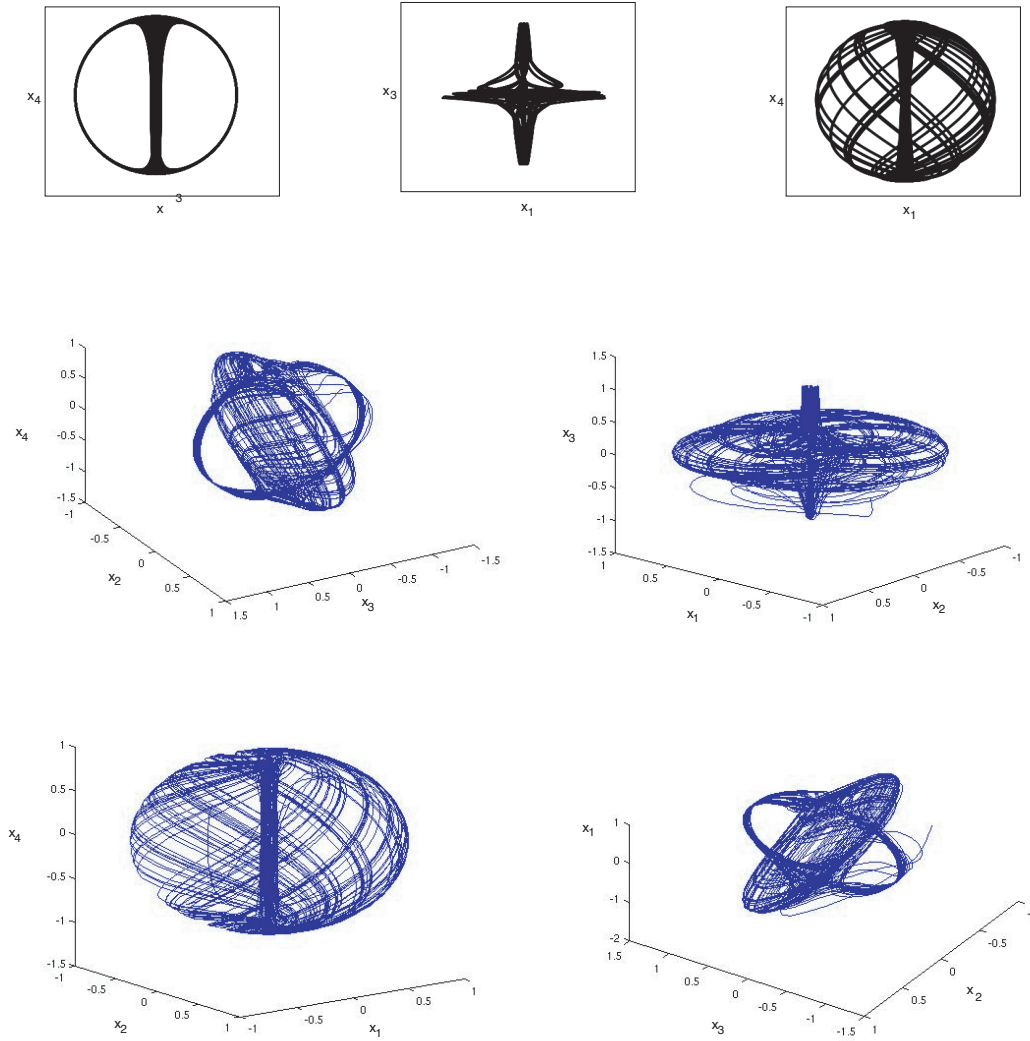


FIGURE 7. The structure of the spiralling set Λ . Top: Projection in the (x_3, x_4) , (x_1, x_3) and (x_1, x_4) -planes of the trajectory with initial condition $(-0.5000, -0.1390, -0.8807, 0.3013)$ for the flow of \mathbf{X}_1 , with $\alpha_1 = 1$, $\alpha_2 = -0.1$ and $\lambda_1 = 0.05$. Centre and Bottom: Projection in the (x_2, x_3, x_4) , (x_1, x_2, x_3) , (x_1, x_2, x_4) and (x_1, x_3, x_4) -hyperplanes of the trajectory with the same initial condition and parameters.

We illustrate the chaotic behaviour in the projected phase portraits of Figure 7 and in the time series of Figure 8 corresponding to a trajectory that stays near the heteroclinic network. Observing Figure 7, it is clear why we call the nonwandering set Λ of \mathbf{X}_1 a *spiralling set*. The time series of Figure 8 also suggests heteroclinic switching: the trajectory follows a sequence of heteroclinic connections in a random order. We stress that this occurs because the $\mathbf{Z}_2(\gamma_2)$ -symmetry has been broken.

Under generic perturbations (not necessarily equivariant), there is still an invariant topological sphere, since \mathbf{S}^3 is normally hyperbolic, and the transverse connections are preserved. The spiralling set presented in Theorem 4 may lose branches, changing its nature. Any compact, positively-invariant neighbourhood of the original heteroclinic network will still be positively-invariant after perturbation and will then contain an uniformly hyperbolic basic set displaying

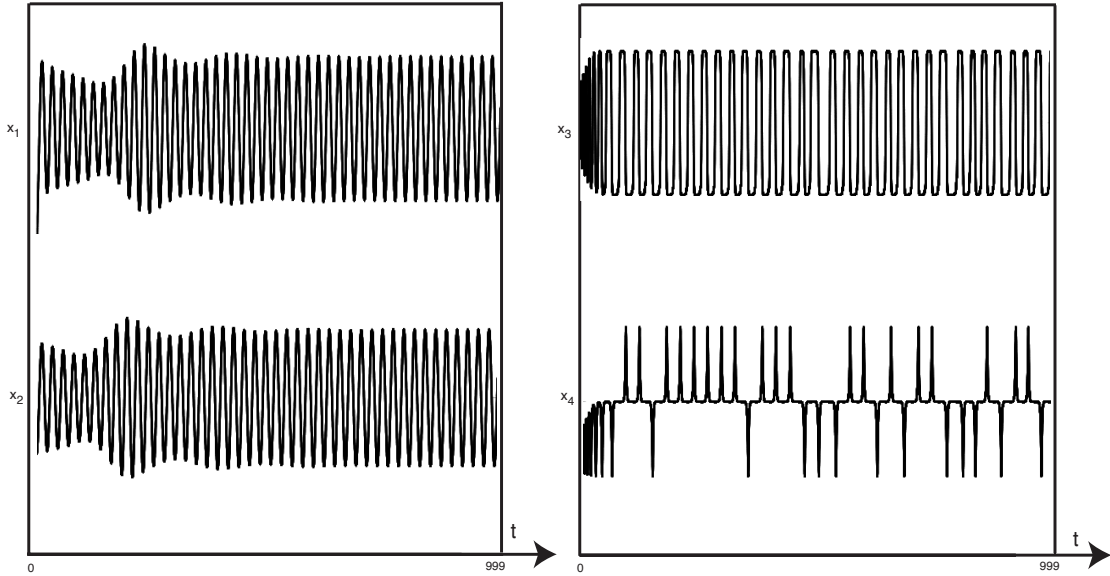


FIGURE 8. Time series for the trajectory with initial condition $(-0.5000, -0.1390, -0.8807, 0.3013)$ for the flow of \mathbf{X}_1 , with $\alpha_1 = 1$, $\alpha_2 = -0.1$ and $\lambda_1 = 0.05$.

structurally stable homoclinic classes in its unfolding, where the results of Rodrigues *et al* [43] may be applied. We will return to this issue in Section 4 below.

3.2.4. Nonhyperbolic behaviour. Based in [31], applying the construction of the proof of Theorem 4 to the unstable manifold of \mathbf{w} , we obtain the following result:

Theorem 7. *There are values λ_1^* of λ_1 arbitrarily close to 0, for which the flow of $\mathbf{X}(X, \lambda_1^*, 0)$ has a heteroclinic tangency between $W^u(\mathbf{w})$ and $W^s(\mathbf{v})$, coexisting with the transverse connections in Σ^* .*

The tangencies of Theorem 7 take place outside the invariant set \mathcal{H} of Theorem 4. Since $E_{\mathbf{v}} < C_{\mathbf{v}}$, Newhouse's results [39, 40] on homoclinic tangencies, extended to heteroclinic tangencies by Hayashi's Connecting Lemma [26], ensure the existence of infinitely many sinks nearby.

Proof. Let V and W be the cylindrical neighbourhoods of each equilibrium point defined in 3.2.1. The unstable manifold $W_{loc}^u(\mathbf{w})$ intersects the whole cylinder wall $I_{\mathbf{v}}^{in}$ (not only the upper part) on a closed curve, as shown in Figure 5. For small $\lambda_1 \neq 0$, the portion of the curve lying in the component of $I_{\mathbf{v}}^{in}$ with $y > 0$ has a point of maximum height that divides it in two components. By Proposition 3, each one of these components is mapped into a helix around $O_{\mathbf{w}}^{out}$. The two helices taken together form a curve with at least one fold point (see Figure 10). Varying λ_1 moves the fold point around $O_{\mathbf{w}}^{out}$, exponentially fast in λ_1 . As λ_1 tends to zero, the fold point will cross $W_{loc}^s(\mathbf{v}) \cap O_{\mathbf{w}}^{out}$ infinitely many times, creating heteroclinic tangencies. \square

Each heteroclinic tangency may be destroyed locally by a small perturbation. As reported in [31], these tangencies correspond to the intersection of the local stable and unstable manifolds of a modified horseshoe with infinitely many slabs, and they may be seen as the product of Cantor sets with the property that the fractal dimension is large. This thickness is essentially due to the existence of infinitely many attracting solutions.

These tangencies coexist with the hyperbolic Cantor set \mathcal{H} and the basins of attraction of the sinks lie in the gaps of \mathcal{H} .

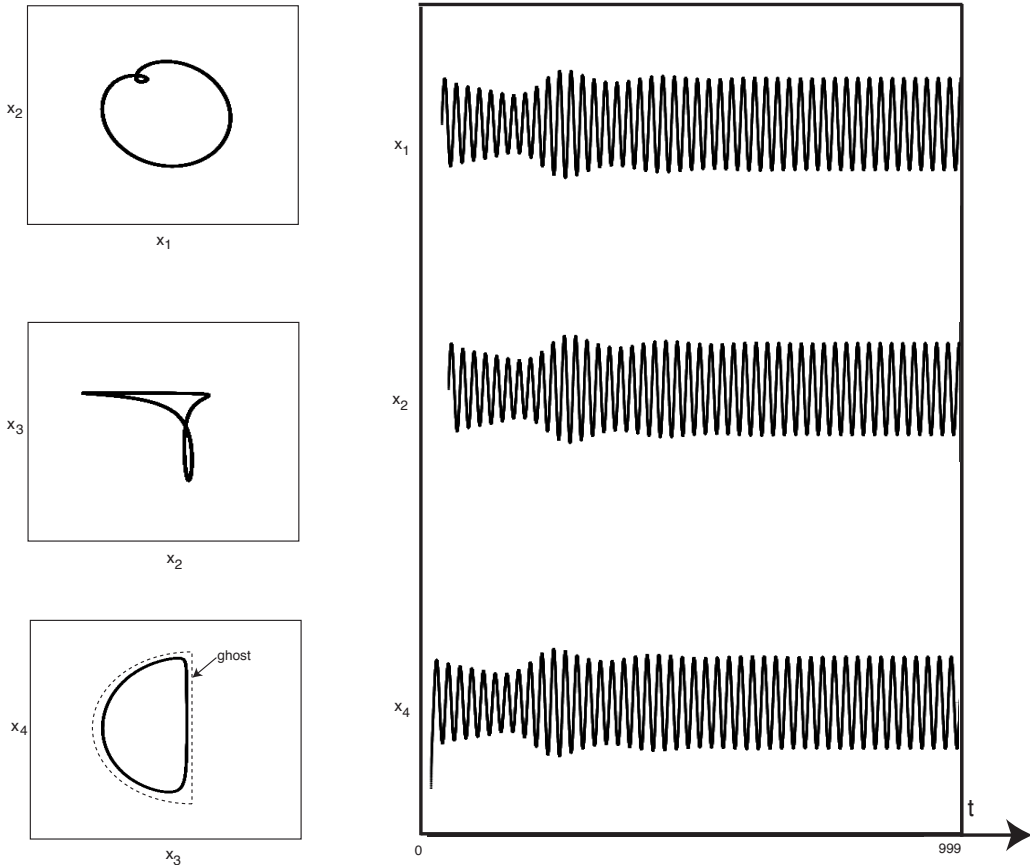


FIGURE 9. Example of a trajectory that accumulates on an attracting periodic orbit. Left: Projection in the (x_1, x_2) , (x_2, x_3) and (x_3, x_4) -planes of the trajectory with initial condition $(-0.5000, -0.1390, -0.8807, 0.3013)$ for the flow corresponding to the equation (2.3), with $\lambda_1 = 0$, $\lambda_2 = 0.05$ for $\alpha_1 = 1$ and $\alpha_2 = -0.1$. The dotted line on the (x_3, x_4) -plane indicates the position of the original cycle. Right: Time series for the corresponding trajectory.

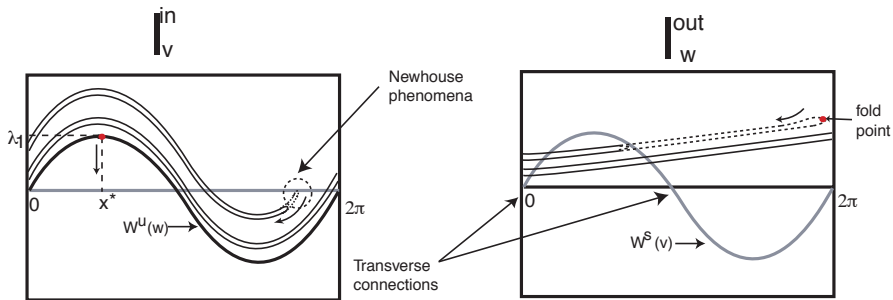


FIGURE 10. Heteroclinic tangency between $W^u(\mathbf{w})$ and $W^s(\mathbf{v})$, coexisting with the transverse connections in Σ^* .

3.3. Breaking the one-dimensional heteroclinic connection. For $\lambda_2 \neq 0$, the vector field $\mathbf{X}_2 = \mathbf{X}(X, 0, \lambda_2)$ is no longer $\mathbf{SO}(2)$ -equivariant but is still equivariant under the action of γ_2 . Since the heteroclinic connections $[\mathbf{v} \rightarrow \mathbf{w}]$ lie on $Fix(\mathbf{Z}_2(\gamma_1))$, these connections disappear,

destroying the heteroclinic network Σ^0 , but for small values of λ_2 there will still be an attractor lying close to the original cycle.

Theorem 6 of [30] shows that for sufficiently small $\lambda_2 \neq 0$, each heteroclinic cycle that occurred in the fully symmetric case is replaced by a stable hyperbolic periodic solution. Using the reflection symmetry γ_2 , two stable periodic solutions co-exist, one in each connected component of $\mathbf{S}^3 \setminus \text{Fix}(\mathbf{Z}_2(\gamma_2))$. Their period tends to $+\infty$ when $\lambda_2 \rightarrow 0$ and their basin of attraction must contain the basin of attraction of Σ^0 . For sufficiently large λ_2 , saddle-node bifurcations of these two periodic solutions occur. Figure 9 illustrates the existence of a single attracting periodic solution in each connected component $\mathbf{S}^3 \setminus \text{Fix}(\mathbf{Z}_2(\gamma_2))$ of the phase space.

4. BREAKING ALL THE SYMMETRY

4.1. Linked homoclinic cycles. In this section, we describe the global bifurcations that are most important for our analysis, which appear when both λ_1 and λ_2 are non-zero and \mathbf{X} has no symmetry. Different chaotic dynamics in (2.3) organise a complex network of bifurcations involving the rotating nodes, that had not yet been considered. The next theorem describes the bifurcation diagram for \mathbf{X} , shown in Figure 11.

Theorem 8. *The germ at the origin of the bifurcation diagram on the (λ_1, λ_2) -plane for $\mathbf{X}(X, \lambda_1 \lambda_2)$ when $\lambda_1 \lambda_2 \neq 0$ satisfies:*

- (1) *For each (λ_1, λ_2) , there is a suspended uniformly hyperbolic horseshoe, topologically conjugate to a full shift over a finite number of symbols. As (λ_1, λ_2) tends to $(\lambda_1, 0)$ with $\lambda_1 \neq 0$, the horseshoe accumulates on the set \mathcal{H} of Theorem 4.*
- (2) *There exists a countable family of open tongues, tangent at $(0, 0)$ to the λ_2 -axis, where \mathbf{X} has an attracting periodic orbit. The closures of these tongues are pairwise disjoint. At the two curves comprising the boundary of each tongue there is an attracting Shilnikov homoclinic connection at \mathbf{v} .*
- (3) *There exists a countable family of open tongues, tangent at $(0, 0)$ to the λ_1 -axis, where \mathbf{X} exhibits a suspended horseshoe, topologically conjugate to a full shift over a finite set of symbols. The closures of these tongues are pairwise disjoint. At the two curves comprising the boundary of each tongue there is an unstable Shilnikov homoclinic connection at \mathbf{w} .*
- (4) *The two sets of curves in the parameter plane described in (2) and (3) meet at isolated points where the two types of homoclinic connections coexist. These codimension two points accumulate at the origin. The closure of the pair of homoclinic orbits forms a link whose linking number tends to infinity as the points approach the origin of the (λ_1, λ_2) -plane.*

Theorem 8 follows from Theorems 7 and 8 in [30]. We present an alternative proof, emphasising the transition between the two different types of chaotic regimes and their geometry. The proof can be carried out for Bykov cycles that are not symmetric. Symmetry is not a deciding factor in the creation of horseshoes, but it makes their existence more natural.

Proof. In Theorem 4, for $\lambda_2 = 0$, we have found a sequence \mathcal{H} of suspended horseshoes contained in the spiralling set Λ . When generic perturbation terms are added, the hyperbolic horseshoes \mathcal{H} lose infinitely many branches, only a finite number of strips survive, as stated in (1).

When $\lambda_1 \neq 0$ and $\lambda_2 = 0$, we have shown in Proposition 3 that a segment β of initial conditions in $I_{\mathbf{v}}^{\text{in}}$, with β transverse to $W^s(\mathbf{v})$, is mapped into a spiral in $I_{\mathbf{w}}^{\text{in}}$ and then into a helix in $O_{\mathbf{w}}^{\text{out}}$ accumulating on $W^u(\mathbf{w})$.

When $\lambda_2 \neq 0$, the one-dimensional connection in the cycle is broken. The spirals in $I_{\mathbf{w}}^{\text{in}}$ are off-centred (case (a) of Figure 12) and will turn only a finite number of times around $W^s(\mathbf{w})$. This is why the suspended horseshoes in assertion (1) have a finite number of strips. Suspended

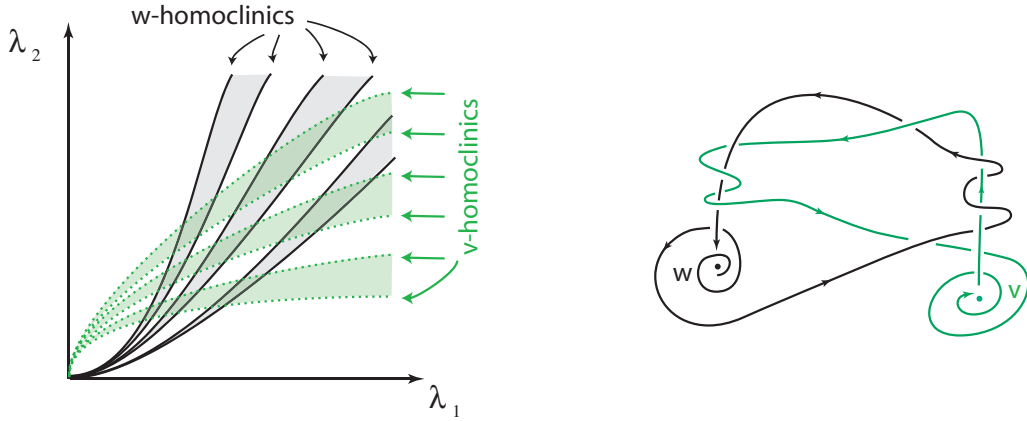


FIGURE 11. Left: Qualitative bifurcation diagram for the family $\mathbf{X}(X, \lambda_1, \lambda_2)$. At the solid curves tangent to the λ_1 axis there is an expanding Shilnikov homoclinic at \mathbf{w} . Consecutive pairs of these curves bound a tongue (shaded) where \mathbf{X} has infinitely many unstable periodic solutions associated to a suspended horseshoe. Contracting Shilnikov homoclinics at \mathbf{v} appear at the dotted curves tangent to the λ_2 axis, that limit tongues where \mathbf{X} has an attracting period orbit. Right: Two linked Shilnikov homoclinic loops appear when the two types of curve meet.

horseshoes arise when $W^u(\mathbf{v})$ is close to $W^s(\mathbf{w}) \cap I_{\mathbf{w}}^{in}$, the number of strips increases as $W^u(\mathbf{v})$ approaches $W^s(\mathbf{w})$.

From the coincidence of the invariant two-dimensional manifolds near the equilibria in the fully symmetric case, we expect that when λ_1 is close to zero, $W^s(\mathbf{v})$ intersects the wall $O_{\mathbf{w}}^{out}$ of the cylinder W in a closed curve as in Figure 5. When both symmetries are broken, the Bykov cycle Σ^* is destroyed, giving rise to Shilnikov homoclinic cycles involving the saddle-foci \mathbf{v} and \mathbf{w} . The equilibria have different Morse indices, thus the dynamics near each homoclinic cycle is qualitatively different, see Shilnikov [47, 48]: all the homoclinic orbits associated to \mathbf{v} are attracting since the contracting eigenvalue is larger than the expanding one. Each homoclinic cycle associated to \mathbf{w} has a suspended horseshoe near it and thus infinitely many periodic solutions of saddle type occur in every neighbourhood of the homoclinicity of \mathbf{w} .

The existence of homoclinic orbits is not a robust property, they occur along the curves in the (λ_1, λ_2) -plane described in assertions (2) and (3) — details on these curves are given in [30, Section 6]. Explicit approximate expressions for these curves may be obtained from the linear part of the vector field, using the transition maps obtained in 3.2.1. At values of (λ_1, λ_2) where the two types of curves cross, as in assertion (4), the homoclinics at \mathbf{v} and \mathbf{w} occur at different regions in phase space.

Case (b) of Figure 12 describes the homoclinic cycle at \mathbf{w} : initially $W^u(\mathbf{w})$ meets $I_{\mathbf{v}}^{in}$ at a closed curve, that is then mapped into a double spiral in $I_{\mathbf{w}}^{in}$ centred at $W^u(\mathbf{v}) \cap I_{\mathbf{w}}^{in}$. When this spiral meets $W^s(\mathbf{w}) \cap I_{\mathbf{w}}^{in}$, an unstable homoclinic cycle associated to \mathbf{w} is created. Similarly, the backwards image of $W^u(\mathbf{v})$ in $O_{\mathbf{w}}^{out}$ is a closed curve, that iterates back into a double spiral in $I_{\mathbf{w}}^{in}$ centred at $W^s(\mathbf{w}) \cap I_{\mathbf{w}}^{in}$, creating an asymptotically stable homoclinic orbit of \mathbf{v} when this spiral meets $W^u(\mathbf{v}) \cap I_{\mathbf{w}}^{in}$. The values of (λ_1, λ_2) where these intersections happen correspond to the two types of curves in Figure 11. The double spiral $W^u(\mathbf{w}) \cap I_{\mathbf{w}}^{in}$ is mapped into a spiral in $O_{\mathbf{w}}^{out}$ as in Figure 12 (c). As one of the spiral arms gets closer to $W^s(\mathbf{w})$ in $I_{\mathbf{w}}^{in}$, its image winds around $O_{\mathbf{w}}^{out}$.

Along the curve in the parameter plane where one of the arms of the double spiral in $W^u(\mathbf{w}) \cap I_{\mathbf{w}}^{in}$ touches $W^s(\mathbf{w}) \cap I_{\mathbf{w}}^{in}$, there are some parameter values where the centre of the spiral in $O_{\mathbf{w}}^{out}$ meets the closed curve $W^s(\mathbf{v}) \cap O_{\mathbf{w}}^{out}$ (Figure 12 (c)). At these points both homoclinic cycles

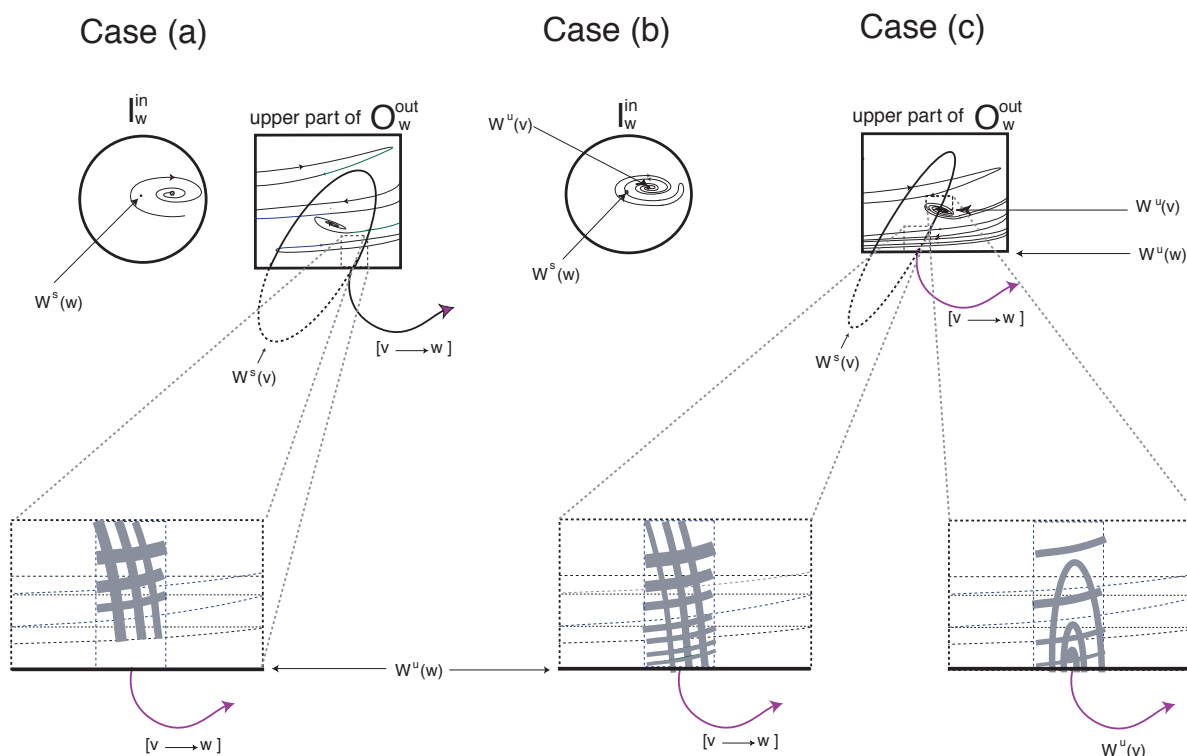


FIGURE 12. There is a sequence of values of λ_2 for which horseshoes with infinitely many *legs* appear and disappear as in a dance, being part of a very complex spiralling network of sets near the ghost of Σ^* . (a) A segment in I_w^{in} transverse to $W^s(\mathbf{v})$ is mapped into a spiral in I_w^{in} . When λ_2 varies, branches of this curve get closer to $W^s(\mathbf{w})$ and its image makes more turns around O_w^{out} , creating horseshoes with more strips. (b) When one of the arms of the double spiral $W^u(\mathbf{w}) \cap I_w^{in}$ touches $W^s(\mathbf{w})$ a homoclinic loop at \mathbf{w} is created. (c) The double spiral $W^u(\mathbf{w}) \cap I_w^{in}$ is mapped into a curve in O_w^{out} that winds a few times around the cylinder and then spirals into a point in $W^u(\mathbf{v})$. A stable homoclinic loop at \mathbf{v} is created when the spiral centre touches the closed curve $W^s(\mathbf{v}) \cap O_w^{out}$. This may happen for the same parameter values that yield the homoclinic at \mathbf{w} .

coexist in different regions of the phase space and the basin of attraction of the homoclinic at \mathbf{v} lies inside the gaps of the suspended horseshoes that appear and disappear from the homoclinicity at \mathbf{w} . \square

We observe a mixing of regular and chaotic dynamics, in regions of parameter space (λ_1, λ_2) where the two types of tongues overlap. Examples of chaotic behaviour of this type should be regarded as quasiattractors due to the presence of stable periodic orbits within them. A lot more needs to be done before these transitions are well understood.

4.2. Finite heteroclinic switching. Generic breaking of the γ_1 -symmetry destroys the heteroclinic network, because the two connections $[\mathbf{v} \rightarrow \mathbf{w}]$ break. Nevertheless, finite switching might be observed: for small values of λ_2 there are trajectories that visit neighbourhoods of finite sequences of nodes. This is because the spirals on top of the cylinder around \mathbf{w} are off-centred and will turn a finite number of times around $W^s(\mathbf{w})$. In this way we may obtain points

whose trajectories follow short finite paths on the network. As $W^u(\mathbf{v})$ gets closer to $W^s(\mathbf{w})$ (as the system moves closer to $\mathbf{Z}_2(\gamma_1)$ symmetry) the paths that can be shadowed get longer.

5. DISCUSSION

The goal of this paper is to construct explicitly a two-parameter family of polynomial differential equations, in which each parameter controls a type of symmetry breaking. We prove analytically the transverse intersection of two invariant manifolds using the adapted Melnikov method which is very difficult in general.

This article uses a systematic method to construct examples of vector fields with simple forms that make their dynamic properties amenable to analytic proof. The method, started in [4], consists of using symmetry to obtain basic dynamics and then choosing special symmetry-breaking terms with a simple form that preserve the required properties, and that introduce some desired behaviour.

Some dynamical properties in this article follow applying results in the literature. We also describe the transition between the different types of dynamics. As far as we know, both the construction and the study of the transition between dynamics are new. This article is also part of a program of systematic study of the dynamics near networks with rotating nodes, together with [30]. The aim of the present article is the study of the non-wandering set that appears in the flow whereas the focus of [30] is the bifurcation diagram. Along this discussion we compare our results to what is known for other models in the literature.

5.1. Shilnikov homoclinic cycles. For three-dimensional flows, one unstable homoclinic cycle of Shilnikov type is enough to predict the existence of a countable infinity of suspended spiralling horseshoes [47, 48]. Their existence does not require breaking the homoclinic connection as in the case of saddles whose linearisation has only real eigenvalues. Under a dissipative condition, strange attractors similar to Λ of Theorem 4 appear in the neighbourhood of a Shilnikov orbit [28]. These attractors are characterised by the lack of uniform hyperbolicity, by the existence of a trajectory with positive Lyapunov exponent and by the existence of an open set in their basin of attraction. Many of the results in this paper are typical of the behaviour in the neighbourhood of a single homoclinic cycle to a saddle-focus, although the dynamics in our case is richer, due to the coexistence of different types of phenomena for the same vector field.

5.2. Bykov cycles. The example presented in this article has an interesting relation with the works of Glendinning and Sparrow [19, 20] about homoclinic cycles and T-points. These authors studied the existence of multiround heteroclinic cycles in a two-dimensional parameter diagram. They found a logarithmic spiral of homoclinic cycles and more complicated Bykov cycles. In their article, these authors do not break the one-dimensional heteroclinic connection. Following the same lines, Bykov [15, 16] studied the codimension 2 case of the same kind of cycle for general systems and found infinitely many periodic solutions and homoclinic cycles of Shilnikov type. Our results differ in some parts from those of Bykov but the similarities are consistent. More precisely, if we allow λ_2 to be a two-dimensional parameter, then for λ_1 fixed, we would find the same type of logarithmic spirals corresponding to homoclinic cycles. Another difference is that Theorem 4 and Corollary 6 do not depend on the ratio of the eigenvalues of the rotating nodes, as is the case in [16].

5.3. Robustly transitive sets. The spiralling set Λ of Theorem 4 is remarkably different from the robustly transitive sets described by Araújo and Pacífico [7] and Morales *et al* [38]. This is easily seen using assertion (3) of Theorem 8 to obtain, for arbitrarily small λ_2 , a homoclinic cycle to \mathbf{w} of Shilnikov type with the expanding eigenvalue greater than the contracting one. This induces the appearance of an arbitrarily large number of attracting and repelling periodic solutions. If Λ were robustly transitive, this would imply that \mathbf{X}_1 could not be C^1 -approximated

by vector fields exhibiting either attracting or repelling sets, which would be a contradiction. Although the spiralling set Λ is not robustly transitive, by Theorem 2 it is persistent under \mathbf{Z}_2 -symmetric perturbations.

5.4. Contracting Lorenz models. The study of these spiralling sets has not attracted as much attention as the Lorenz attractor because, in general, it is difficult to understand the topology associated to non-real eigenvalues. The fact that these wild spiral sets contain equilibria makes them similar to Lorenz-like attractors described by Rovella [45]. Both examples show suspended horseshoes, coexisting with equilibria and periodic solutions.

In our example, suspended horseshoes are present for an open set of parameters whereas in Rovella's example they appear for a set of parameters with positive Lebesgue measure. Moreover, in our example, the suspended horseshoes coexist with heteroclinic tangencies and these in turn give rise to attracting periodic orbits, whose basins of attraction may be situated in the gaps of the horseshoes accumulating on the repelling original Bykov cycle [41]. The attractor splits into infinitely many components, whereas Rovella's example satisfies Axiom A for a set of parameters with positive Lebesgue measure.

5.5. Quasistochastic attractors. The features of our example fit in the properties of the *quasistochastic attractors* studied by Gonchenko *et al* [22]. The tangencies proved in Theorem 7 give rise to attracting periodic solutions which coexist with the hyperbolic set \mathcal{H} ; the basins of attraction of some sinks lie in the gaps of \mathcal{H} . The transitive non-isolated set Λ surrounds closed trajectories of different indices, in sharp contrast to what is expected of attractors that are either hyperbolic or Lorenz-like.

Yet another feature that differs from hyperbolic sets is that Λ should not possess the property of *self-similarity*. There may exist infinitely many time scales on which behavior of the system is qualitatively different. We would like to stress that our attracting limit set Λ , composed by unstable orbits, may support proper invariant measures (Sinai-Bowen-Ruelle measures) and, therefore, it may be studied in ergodic terms.

A generic perturbation of the partially symmetric vector field \mathbf{X}_1 still has some spiralling structure as reported in [8, 9]. It contains a finite sequence of topological horseshoes semiconjugate to full shifts over an alphabet with a finite number of symbols, instead of an infinite sequence. We believe that our example should be explored further because it puts together different phenomena. The two different types of chaos reported in [44] have been observed in Theorem 8 and Figure 12. The behaviour near these specific networks can be lifted to larger networks as those reported in [6, 22, 42, 43].

5.6. Final Remarks. The properties of the family \mathbf{X} that we have described depend strongly on the orientation around the heteroclinic connection $[\mathbf{v} \rightarrow \mathbf{w}]$. If the rotations inside V and inside W had opposite orientations, for some trajectories these two rotations in V and W would cancel out. The Bykov cycle would no longer be repelling. Newhouse phenomena are dense in a Bykov cycle of this type, and hence infinitely many strange attractors emerge. A systematic study of this case is in preparation using the concept of *chirality*.

A lot more needs to be done before we understand well the dynamics of systems close to symmetry involving rotating nodes. Besides the interest of the study of the dynamics arising in generic unfoldings of an attracting heteroclinic network, its analysis is important because in the fully non-equivariant case the explicit analysis of the first return map seems intractable. Although the symmetry is not essential, in this article we were able to predict qualitative features because the non-symmetric dynamics is close to symmetry.

Acknowledgements: The authors would like to express their gratitude to Manuela Aguiar (University of Porto) for helpful discussions at the beginning of this work. Also special thanks

to Maria Luísa Castro (University of Porto) for the numerical simulations in *Matlab* shown in figure 7.

APPENDIX A. TRANSVERSALITY OF INVARIANT MANIFOLDS

A.1. Melnikov method revisited. Melnikov [36] studied a method to find the transverse intersection of the the invariant manifolds for a time periodic perturbation of a homoclinic cycle. The pioneer idea of Melnikov is to make use of the globally computable solutions of the unperturbed system the computation of perturbed solutions. We start this appendix with a short description of this theory applied to saddle-connections. For a detailed proof for the homoclinic case, see Guckenheimer and Holmes [23, section 4.5].

If $X \in \mathbf{R}^2$, $t \in \mathbf{R}$ and $0 < \varepsilon \ll 1$, consider the planar system:

$$(A.6) \quad \dot{X} = f(X) + \varepsilon g(X, t)$$

such that:

- there exists $T > 0$ such that $g(X, t) = g(X, t + T)$ for all t ie g is T -periodic;
- for $\varepsilon = 0$, the flow has a heteroclinic connection Γ_0 associated to two hyperbolic points p_0 and p_1 ;
- the unstable manifold of p_0 coincides with the stable manifold of p_1 .

Associated to the system (A.6), taking $\mathbf{S}^1 \cong \mathbf{R}/T$, we define the suspended system:

$$\dot{X} = f(X) + \varepsilon g(X, \theta), \quad \dot{\theta} = 1, \quad (X, \theta) \in \mathbf{R}^2 \times \mathbf{S}^1.$$

With the above assumptions, $\{p_0\} \times \mathbf{S}^1$ and $\{p_1\} \times \mathbf{S}^1$ are hyperbolic periodic solutions for the suspended flow, whose invariant manifolds $\Gamma_0 \times \mathbf{S}^1$ coincide. Since the limit cycles are hyperbolic, their hyperbolic continuation is well defined for $\varepsilon \neq 0$; hereafter we denote them by $\{p_0^\varepsilon\} \times \mathbf{S}^1$ and $\{p_1^\varepsilon\} \times \mathbf{S}^1$. Under general conditions (without symmetry for example), the heteroclinic connection $\Gamma_0 \times \mathbf{S}^1$ is not preserved and for a non-empty open set in the parameter space, the invariant manifolds meet transversely. Their intersection consists of a finite number of trajectories.

On a transverse cross section to the perturbed system, the splitting of the stable and unstable manifolds is measured by the *Melnikov function*:

$$(A.7) \quad M(t_0) = \int_{-\infty}^{+\infty} f(q_0(t)) \wedge g(q_0(t), t + t_0) \cdot \exp\left(-\int_0^t \text{tr} Df(q_0(s)) ds\right) dt,$$

where $q_0(t)$ is the parametrisation of the solution of the unperturbed system (A.6) starting at $t_0 = 0$ on Γ_0 . Recall that the *wedge product* in \mathbf{R}^2 of two vectors (u_1, u_2) and (v_1, v_2) is simply given by $u_1 v_2 - u_2 v_1$. When f is hamiltonian, then $\text{tr} Df(q_0(t)) = 0$ and the expression for the Melnikov function is simpler. The main result we will use is the following:

Theorem 9 (Bertozi [14], Melnikov [36], adapted). *Under the above conditions, and for $\varepsilon > 0$ sufficiently small, if $M(t_0)$ has simple zeros, then $W^u(p_0^\varepsilon)$ and $W^s(p_1^\varepsilon)$ intersect transversely .*

This result is important because it allows to prove the existence of transverse (and hence robust) homo and heteroclinic connections as we proceed to do.

A.2. Proof of transversality.

Theorem 10. *If $\lambda_1 \neq 0$ and $\lambda_2 = 0$, the two-dimensional invariant manifolds of the equilibria \mathbf{w} and \mathbf{v} of $\mathbf{X}(X, \lambda_1 \lambda_2)$ intersect transversely in \mathbf{S}^3 along one-dimensional orbits.*

Proof. In spherical coordinates

$$x_1 = r \sin \phi \sin \theta \cos \varphi \quad x_2 = r \sin \phi \sin \theta \sin \varphi \quad x_3 = r \cos \phi \sin \theta \quad x_4 = r \cos \theta$$

equations (2.3) restricted to \mathbf{S}^3 can be written as:

$$(A.8) \quad \begin{aligned} \dot{\theta} &= \alpha_1 \sin \theta \cos(2\phi) + \frac{\alpha_2}{2} \sin(2\theta) + \frac{\lambda_1}{2} \sin^2(\phi) \sin^2(\theta) \cos(\phi) \sin(2\varphi) \\ \dot{\phi} &= -\alpha_1 \cos(\theta) \sin(2\phi) - \frac{\lambda_1}{4} \sin^3(\phi) \sin(2\theta) \sin(2\varphi) \\ \dot{\varphi} &= 1 \end{aligned}$$

From the equation $\dot{\varphi} = 1$, we get $\varphi(t) = t$, $t \in \mathbf{R}$ and (A.8) is reduced to a three-dimensional non-autonomous differential equation of the form:

$$\begin{aligned} \dot{\theta} &= f_1(\theta, \phi) + \lambda_1 g_1(\theta, \phi, t) \\ \dot{\phi} &= f_2(\theta, \phi) + \lambda_1 g_2(\theta, \phi, t) \end{aligned}$$

where

$$\begin{aligned} f_1(\theta, \phi) &= \alpha_1 \sin \theta \cos(2\phi) + \frac{\alpha_2}{2} \sin(2\theta) & f_2(\theta, \phi) &= -\alpha_1 \cos(\theta) \sin(2\phi) \\ g_1(\theta, \phi, t) &= \frac{1}{2} \sin^2(\phi) \sin^2(\theta) \cos(\phi) \sin(2t) & g_2(\theta, \phi, t) &= -\frac{1}{4} \sin^3(\phi) \sin(2\theta) \sin(2t) . \end{aligned}$$

The maps g_1 and g_2 are periodic in t of period π . For the Melnikov function $M(t_0)$ defined in (A.7) we write $f = (f_1, f_2)$ and $g = (g_1, g_2)$. The parametrisation $q_0(t)$ of the connection $[\mathbf{w} \rightarrow \mathbf{v}]$ in the unperturbed system, $\lambda_1 = 0$, is defined by $\phi = \frac{\pi}{2} + k\pi$, $k \in \{0, 1\}$. Thus, in the unperturbed system, the connections $[\mathbf{w} \rightarrow \mathbf{v}]$ are parametrised by:

$$q_0^1(t) = \left(\theta(t), \frac{\pi}{2} \right) \text{ and } q_0^2(t) = \left(\theta(t), \frac{3\pi}{2} \right).$$

Therefore, for $k \in \{0, 1\}$, we have:

$$\begin{aligned} f_1(q_0^i(t)) &= (-1)^k \alpha_1 \sin(\theta(t)) + \frac{\alpha_2}{2} \sin(2\theta(t)) & f_2(q_0^i(t)) &= 0 \\ g_1(q_0^i(t), t + t_0) &= 0 & g_2(q_0^i(t), t + t_0) &= (-1)^{k+1} \frac{1}{4} \sin(2\theta(t)) \sin(2(t + t_0)) . \end{aligned}$$

To see that the integral $M(t_0)$ converges, note that the exterior product in the definition of the Melnikov function $M(t_0)$ is bounded since it is given by:

$$\begin{aligned} f(q_0^i(t)) \wedge g(q_0^i(t), t + t_0) &= \\ &= \left[-\alpha_1 \sin(\theta(t)) + (-1)^{k+1} \frac{\alpha_2}{2} \sin(2\theta(t)) \right] \frac{1}{4} \sin(2\theta(t)) \sin(2(t + t_0)) \end{aligned}$$

and

$$(A.9) \quad \text{tr} Df(q_0(s)) = \alpha_1 \cos(\theta(s)) + \alpha_2 \cos(2\theta(s))$$

hence the Melnikov integral $M(t_0)$ does not depend on λ_1 . Since it has been shown in Aguiar *et al* [4, Lemma 16] that for any $r > 0$, the integral

$$\int_{-\infty}^{+\infty} \exp \left(- \int_0^t \alpha_2 r \cos(\theta(s)) + \alpha_3 r^2 \cos(2\theta(s)) ds \right) dt$$

converges, the convergence of $M(t_0)$ follows. It remains to prove that the roots of $M(t_0)$ exist and are simple, completing the proof of Theorem 10. This is the content of next lemma whose proof is similar to results in [4]. \square

Lemma 11. *The Melnikov integral $M(t_0)$ has simple roots.*

Proof. Using the expression (A.9) and the expression of the sin of the sum, we may write $M(t_0)$ in the form:

$$M(t_0) = \cos(2t_0) \int_{-\infty}^{+\infty} [\sin(2t)] E(t) dt + \sin(2t_0) \int_{-\infty}^{+\infty} [\cos(2t)] E(t) dt$$

where

$$E(t) = \left[-\alpha_1 \sin(\theta(t)) + (-1)^{k+1} \frac{\alpha_2}{2} \sin(2\theta(t)) \right] \left[\frac{1}{4} \sin(2\theta(t)) \right] \exp(-\text{tr} Df(q_0(s))).$$

Suppose that t_0 is a non-simple zero of $M(t_0)$. Since t_0 is a zero, then:

$$(A.10) \quad \cos(2t_0) \int_{-\infty}^{+\infty} [\sin(2t)]E(t)dt + \sin(2t_0) \int_{-\infty}^{+\infty} [\cos(2t)]E(t)dt = 0,$$

or equivalently

$$\tan(2t_0) = -\frac{\int_{-\infty}^{+\infty} \sin(2t)E(t)dt}{\int_{-\infty}^{+\infty} \cos(2t)E(t)dt}.$$

Since t_0 is non-simple, differentiating (A.10) with respect to t_0 we must have:

$$-\sin(2t_0) \int_{-\infty}^{+\infty} [\sin(2t)]E(t)dt + \cos(2t_0) \int_{-\infty}^{+\infty} [\cos(2t)]E(t)dt = 0,$$

and thus:

$$\tan(2t_0) = \frac{\int_{-\infty}^{+\infty} \cos(2t)E(t)dt}{\int_{-\infty}^{+\infty} \sin(2t)E(t)dt},$$

which is a contradiction. It remains to show that $M(t_0)$ has at least a zero. For this purpose, write:

$$\rho \exp(-i\varsigma) = \int_{-\infty}^{+\infty} \exp(-2it)E(t) \quad \text{whence} \quad M(t_0) = \rho \operatorname{Re}(\exp(i(2t_0 - \varsigma))).$$

Thus $M(t_0)$ has zeros at $t_0 = \frac{1}{4}(\pi + 2\varsigma + 2n\pi)$, $n \in \mathbf{Z}$. □

APPENDIX B. SYMMETRY BREAKING PERTURBATIONS

List of homogeneous polynomial vector fields of degree 3, tangent to \mathbf{S}^3 and their symmetries in $\mathbf{SO}(\mathbf{2}) \times \mathbf{Z}_2(\gamma_2)$, that may be used for perturbations as in section 2.3. Adapted from Aguiar [3].

Perturbing terms with $\mathbf{SO}(\mathbf{2}) \times \mathbf{Z}_2(\gamma_2)$ -symmetry:

$$(x_2x_4^2, -x_1x_4^2, 0, 0) \quad (x_2x_3^2, -x_1x_3^2, 0, 0) \quad (0, 0, x_3x_4^2, -x_3^1x_4)$$

Perturbing terms with $\mathbf{SO}(\mathbf{2})$ -symmetry, not $\mathbf{Z}_2(\gamma_2)$ -symmetric:

$$(0, 0, x_4^3, -x_3x_4^2) \quad (x_2x_3x_4, -x_1x_3x_4, 0, 0) \quad (0, 0, x_3^2x_4, -x_3^3)$$

Perturbing terms with $\mathbf{Z}_2(\gamma_1) \times \mathbf{Z}_2(\gamma_2)$ -symmetry, not $\mathbf{SO}(\mathbf{2})$ -symmetric:

$$\begin{array}{cccc} (x_1^2x_2, -x_1^3, 0, 0) & (x_2^3, -x_1x_2^2, 0, 0) & (0, x_1x_4^2, 0, -x_1x_2x_4) & (x_1x_4^2, 0, 0, -x_1^2x_4) \\ (x_2x_3^2, 0, -x_1x_2x_3, 0) & (0, x_1x_3^2, -x_1x_2x_3, 0) & (0, x_2x_3^2, -x_2^2x_3, 0) & (x_1x_2^2, -x_1^2x_2, 0, 0) \\ (x_2x_4^2, 0, 0, -x_1x_2x_4) & (0, x_2x_4^2, 0, -x_2^2x_4) & (x_1x_3^2, 0, -x_1^2x_3, 0) & \end{array}$$

Perturbing terms with $\mathbf{Z}_2(\gamma_1)$ -symmetry, not $\mathbf{SO}(\mathbf{2})$ -symmetric nor $\mathbf{Z}_2(\gamma_2)$ -symmetric:

$$\begin{array}{cccc} (0, 0, x_1x_2x_4, -x_1x_2x_3) & (0, x_2x_3x_4, 0, -x_2^2x_3) & (x_1x_2x_3, -x_1^2x_3, 0, 0) & (0, 0, x_1^2x_4, -x_1^2x_3) \\ (0, x_1x_3x_4, -x_1x_2x_4, 0) & (0, x_1x_3x_4, 0, -x_1x_2x_3) & (0, x_2x_3x_4, -x_2^2x_4, 0) & (x_2x_3x_4, 0, -x_1x_2x_4, 0) \\ (x_2x_3x_4, 0, 0, -x_1x_2x_3) & (0, 0, x_2^2x_4, -x_2^2x_3) & (x_1x_3x_4, 0, -x_1^2x_4, 0) & (x_1x_3x_4, 0, 0, -x_1^2x_3) \end{array}$$

Perturbing terms with $\mathbf{Z}_2(\gamma_2)$ -symmetry, not $\mathbf{SO}(\mathbf{2})$ -symmetric nor $\mathbf{Z}_2(\gamma_1)$ -symmetric:

$$\begin{array}{cccc} (x_3^2x_4, 0, -x_1x_3x_4, 0) & (0, x_1^2x_4, 0, -x_1^2x_2) & (x_2^2x_4, -x_1x_2x_4, 0, 0) & (0, x_2^2x_4, 0, -x_2^3) \\ (0, x_3^2x_4, 0, -x_2x_3^2) & (x_2^2x_4, 0, 0, -x_1x_2^2) & (x_3^2x_4, 0, 0, -x_1x_3^2) & (0, x_3^2x_4, -x_2x_3x_4, 0) \\ (x_1^2x_4, 0, 0, -x_1^3) & (x_1x_2x_4, -x_1^2x_4, 0, 0) & (0, x_1x_2x_4, 0, -x_1x_2^2) & (0, 0, 0, x_1x_3x_4, -x_1x_3^2) \\ (x_4^3, 0, 0, -x_1x_4^2) & (x_1x_2x_4, 0, 0, -x_1^2x_2) & (0, 0, x_2x_3x_4, -x_2x_3^2) & (0, x_4^3, 0, -x_2x_4^2) \end{array}$$

Perturbing terms without any of the symmetries above:

$$\begin{array}{cccc}
 (x_1x_2x_3, 0, -x_1^2x_2, 0) & (x_3x_4^2, 0, 0, -x_1x_3x_4) & (0, x_3^3, -x_2x_3^2, 0) & (x_1^2x_3, 0, -x_1^3, 0) \\
 (0, x_1^2x_3, -x_1^2x_2, 0) & (x_2^2x_3, -x_1x_2x_3, 0, 0) & (0, 0, x_1x_4^2, -x_1x_3x_4) & (0, x_3x_4^2, 0, -x_2x_3x_4) \\
 (x_2^2x_3, 0, -x_1x_2^2, 0) & (0, 0, x_2x_4^2, -x_2x_3x_4) & (0, x_1x_2x_3, -x_1x_2^2, 0) & (x_3^3, 0, -x_1x_2^3, 0) \\
 (x_3x_4^2, 0, -x_1x_4^2, 0) & (0, x_2^2x_3, -x_2^3, 0) & (0, x_3x_4^2, -x_2x_4^2, 0) &
 \end{array}$$

REFERENCES

[1] V. S. Afraimovich, V. V. Bykov, L. P. Shilnikov, *On the appearance and structure of the Lorenz attractor*, Dokl. Acad. Sci. USSR, No. 234, 336–339, 1977

[2] V. S. Afraimovich, S. C. Chow, W. Liu, *Lorenz-type attractors from codimension one bifurcation*, J. Dynam. Differential Equations, Vol. 7(2), 375–407, 1995

[3] M. A. D. Aguiar, *Vector Fields with Heteroclinic Networks*, PhD thesis, University of Porto, Portugal, 2002

[4] M. A. D. Aguiar, S. B. S. D. Castro, I. S. Labouriau, *Simple Vector Fields with Complex Behaviour*, Int. Jour. of Bifurcation and Chaos, Vol. 16 (2), 369–381, 2006

[5] M. A. D. Aguiar, S. B. S. D. Castro, I. S. Labouriau, *Dynamics near a heteroclinic network*, Nonlinearity 18, 391–414, 2005

[6] M. A. D. Aguiar, I. S. Labouriau, A. A. P. Rodrigues, *Switching near a heteroclinic network of rotating nodes*, Dynamical Systems: an International Journal, 25 (1), 75–95, 2010

[7] V. Araújo, M. J. Pacifico, *Three dimensional flows*, Ergebnisse der Mathematik und ihrer Grenzgebiete, Vol. 53, Springer, Berlin, Heidelberg, 2010

[8] A. Arneodo, P. Couillet, C. Tresser, *A possible new mechanism for the onset of turbulence*, Phys. Lett. A 81, 197–201, 1981

[9] A. Arneodo, P. Couillet, C. Tresser, *Possible new strange attractors with spiral structure*, Comm. Math. Phys. 79, 573–579, 1981

[10] A. Arroyo, F. Rodriguez-Hertz, *Homoclinic bifurcations and uniform hyperbolicity for three-dimensional flows*, Ann. Inst. H. Poincaré Anal. Non Linéaire, No. 20, 805–841, 2003

[11] M. A. Aziz-Alaoui, *Differential Equations with Multispiral Atractors*, Int. Journ. of Bifurcation and Chaos, No. 9, Issue 6, 1009–1039, 1999

[12] S. Bautista, *Sobre conjuntos hiperbólicos singulares*, Ph.D. Thesis, IM.UFRJ, Rio de Janeiro, 2005

[13] J. B. Berg, S. A. Gils, T.P.P. Visser, *Parameter dependence of homoclinic solutions in a single long Josephson junction*, Nonlinearity 16, 707–717, 2003

[14] A. L. Bertozzi, *Heteroclinic orbits and chaotic dynamics in planar fluid flows*, SIAM J. Math. Anal, Vol. 19, No. 6, 1271–1294, 1988

[15] V. V. Bykov, *The bifurcations of separatrix contours and chaos*, Phys. D, 62, 290–299, 1993

[16] V. V. Bykov, *Orbit structure in a neighborhood of a separatrix cycle containing two saddle-foci*, Amer. Math. Soc. Transl. 200, 87–97, 2000

[17] J. H. P. Dawes, *Hopf bifurcation on a square superlattice*, Nonlinearity 14, 491–511, 2001

[18] M. J. Field, *Lectures on bifurcations, Dynamics and Symmetry*, Pitman Research Notes in Mathematics Series vol 356, Harlow: Longman 1996

[19] P. Glendinning, C. Sparrow, *Local and Global Behaviour near Homoclinic Orbits*, J. Stat. Phys., 35, 645–696, 1984

[20] P. Glendinning, C. Sparrow, *T-points: a codimension two heteroclinic bifurcation*, J. Stat. Phys., 43, 479–488, 1986

[21] M. Golubitsky, I. Stewart, *The Symmetry Perspective*, Birkhauser, 2000

[22] S. V. Gonchenko, L. P. Shilnikov, D. V. Turaev, *Dynamical phenomena in systems with structurally unstable Poincare homoclinic orbit*, Chaos 6(1), 15–31, 1996

[23] J. Guckenheimer, P. Holmes, *Nonlinear Oscillations, Dynamical Systems, and Bifurcations of Vector Fields*, Applied Mathematical Sciences, No. 42, Springer-Verlag, 1983

[24] J. Guckenheimer, P. Worfolk, *Instant Chaos*, Nonlinearity 5, 1211–1222, 1991

[25] J. Guckenheimer, R. F. Williams, *Structural stability of Lorenz attractors*, Publ. Math. IHES, No. 50, 59–72, 1979

[26] S. Hayashi, *Connecting invariant manifolds and the solution of the C^1 -stability and Ω -stability conjectures for flows*, Ann. of Math. 2, 145(1), 81–137, 1997

[27] P. Holmes, *A strange family of three-dimensional vector fields near a degenerate singularity*, J. Diff. Eqns, 37, 382–403, 1980

[28] A. J. Homburg, *Periodic attractors, strange attractors and hyperbolic dynamics near homoclinic orbit to a saddle-focus equilibria*, Nonlinearity 15, 411–428, 2002

- [29] I. S. Labouriau, A. P. Dias, *Instant chaos is chaos in slow motion*, Journal of Mathematical Analysis and Applications, 199-2, 138–148, 1996
- [30] I. S. Labouriau, A. A. P. Rodrigues, *Global Generic Dynamics close to Symmetry*, Journal of Differential Equations, 253, 2527–2557, 2012
- [31] I. S. Labouriau, A. A. P. Rodrigues, *Partial Symmetry Breaking and Heteroclinic Tangencies*, Proceedings in Mathematics and Statistics — Progress and challenges in dynamical systems, (to appear), 2013
- [32] E. N. Lorenz, *Deterministic nonperiodic flow*, J. Atmosph. Sci., No. 20, 130–141, 1963
- [33] H. Kokubu, R. Roussarie, *Existence of a singularly degenerate heteroclinic cycle in the Lorenz system and its dynamical consequences*, I. J. Dynam. Differential Equations, 9, 445–462, 1997
- [34] M. Krupa, I. Melbourne, *Asymptotic Stability of Heteroclinic Cycles in Systems with Symmetry*, Ergodic Theory and Dynam. Sys., Vol. 15, 121–147, 1995
- [35] M. Krupa, I. Melbourne, *Asymptotic Stability of Heteroclinic Cycles in Systems with Symmetry, II*, Proc. Roy. Soc. Edinburgh, 134A, 1177–1197, 2004
- [36] V. K. Melnikov, *On the stability of the center for time-periodic perturbations*, Trans. Moscow Math. Soc., Number 12, 1–57, 1963
- [37] C. A. Morales, *Lorenz attractor through saddle-node bifurcations*, Ann. Inst. H. Poincaré Anal. Non Linéaire, 13, No. 5, 589–617, 1996
- [38] C. A. Morales, M. J. Pacífico, E. R. Pujals, *Robust transitive singular sets for 3-flows are partially hyperbolic attractors or repellers*, Ann. of Math., No. 2, Vol. 160, 375–432, 2004
- [39] S.E. Newhouse, *Diffeomorphisms with infinitely many sinks*, Topology 13 9–18, 1974
- [40] S.E. Newhouse, *The abundance of wild hyperbolic sets and non-smooth stable sets for diffeomorphisms*, Publ. Math. Inst. Hautes Etudes Sci. 50, 101–151, 1979
- [41] A. A. P. Rodrigues, *Repelling dynamics near a Bykov cycle*, Journal of Dynamics and Differential Equations, Vol. 25–3, 605–625, 2013
- [42] A. A. P. Rodrigues, *Persistent Switching near a Heteroclinic Model for the Geodynamo Problem*, Chaos, Solitons & Fractals, Vol. 47, 73–86, 2013
- [43] A. A. P. Rodrigues, I. S. Labouriau, M. A. D. Aguiar, *Chaotic Double Cycling*, Dynamical Systems: an International Journal, Vol. 26–2, 199–233, 2011
- [44] O. E. Rossler, *Different types of chaos in two simple differential equations*, Zeitschrift für Naturforsch A, 31, 1664–1670, 1976
- [45] A. Rovella, *The dynamics of perturbations of contracting Lorenz maps*, Bol. Soc. Brasil. Mat. No. 24, 233–259, 1993
- [46] V. S. Samovol, *Linearization of a system of differential equations in the neighbourhood of a singular point*, Sov. Math. Dokl, Vol. 13, 1972
- [47] L. Shilnikov, *A case of the existence of a denumerable set of periodic motions*, Sov. Math. Dokl. 6, 163–166, 1965
- [48] L. Shilnikov, *On the generation of a periodic motion from trajectories doubly asymptotic to an equilibrium state of saddle type*, Math. USSR Sbornik 77(119), 461–472, 1968

CENTRO DE MATEMÁTICA DA UNIVERSIDADE DO PORTO, AND FACULDADE DE CIÊNCIAS, UNIVERSIDADE DO PORTO, RUA DO CAMPO ALEGRE, 687, 4169-007 PORTO, PORTUGAL

E-mail address, A.A.P. Rodrigues: alexandre.rodrigues@fc.up.pt

E-mail address, I.S. Labouriau: islabour@fc.up.pt